

Parametric Studies on Triangular Tension Leg Platform

by

ABDUL HAZEEM BIN HAMZAH

8100

Dissertation submitted in partial fulfilment of
the requirement for the
Bachelor of Engineering (Hons)
(Civil Engineering)

JUNE 2010

Supervisor:

Mr. Mohamed Mubarak Bin Abdul Wahab

Universiti Teknologi Petronas
Bandar Seri Iskandar
31750 Tronoh
Perak Darul Ridzuan

CERTIFICATION OF APPROVAL

Parametric Studies on Triangular Tension Leg Platform

by

Abdul Hazeem Bin Hamzah

A project dissertation submitted to the
Civil Engineering Programme
Universiti Teknologi PETRONAS
in partial fulfilment of the requirement for the
Bachelor of Engineering (Hons)
(Civil & Electronics Engineering)

Approved:



Mohamed Mubarak Bin Abdul Wahab
Project Supervisor

UNIVERSITI TEKNOLOGI PETRONAS
TRONOH, PERAK

June 2010

CERTIFICATION OF ORIGINALITY

This is to certify that I am responsible for the work submitted in this project, that the original work is my own except as specified in the references and acknowledgements, and that the original work contained herein have not been undertaken or done by unspecified sources or persons.

A handwritten signature in black ink, appearing to read 'Abdul Hazeem Bin Hamzah', written over a horizontal line.

Abdul Hazeem Bin Hamzah

ABSTRACT

Tension Leg Platform (TLP) is a buoyant platform held in place by mooring system. TLP's are similar to conventional fixed platforms except that the platform is maintained on location through the use of moorings held in tension by the buoyancy of the hull. The cost for TLP increases with the water depth. More studies are going on to find solution to reduce the cost on TLP design. This study focuses on the influence of energy spectrum model on the triangular TLP. Pierson-Moskowitz (PM) and JONSWAP spectrum were used in this study. Wave forces were estimated at the instantaneous position of the platform by Morison's equation with Airy's linear wave theory. Wave is considered to act unidirectional in the surge direction only. All forces acting on the platform were calculated to determine the TLP's response in surge, heave and pitch degrees of freedom. Lab test had been done to support and justify the motion response calculated in the numerical calculation. As a conclusion, only a small significant difference in surge, heave and pitch motion response distance for both PM and JONSWAP energy spectrums, but the frequencies of the TLP motion on surge, heave and pitch degree of freedom can effects the TLP tethers.

ACKNOWLEDGEMENT

I am heartily thankful to my supervisor, Mr. Muhamed Mubarak and my co-supervisor; Prof. Dr. Kurian v. John, whose encouragement, guidance and support from the initial to the final level enabled me to develop an understanding of the subject. It is a pleasure to thank those who made this research possible. I am indebted to my parent and many of my colleagues to support me in completing this research.

Lastly, I offer my regards and blessings to all of those who supported me in any respect during the completion of the project.

TABLE OF CONTENTS

CERTIFICATION OF APPROVAL.....	i
CERTIFICATION OF ORIGINALITY.....	ii
ABSTRACT.....	iii
ACKNOWLEDGEMENT.....	iv
TABLE OF CONTENTS.....	v
LIST OF FIGURES.....	vii
LIST OF TABLES.....	viii
CHAPTER 1 INTRODUCTION.....	1
1.1 Background of Study.....	1
1.2 Problem Statement.....	2
1.3 Objectives	3
1.4 Project Scope and Overview.....	4
CHAPTER 2 LITERATURE REVIEW.....	5
2.1 Tension Leg Platform.....	5
2.1.1 TLP Foundation.....	6
2.1.2 TLP Shape and Hydrodynamic Coefficients.....	6
2.1.3 TLP Tethers.....	8
2.1.4 TLP Behaviour under Random Wave.....	8
2.1.5 TLP Behaviour under Impact Loading.....	9
2.2 Wave Spectrum Models.....	9
CHAPTER 3 METHODOLOGY.....	11
3.1 Dimensional, Structural and Environmental Data.....	11
3.2 Numerical Studies.....	13
3.2.1 Assumption.....	13
3.2.2 Force Calculation.....	13
3.2.3 Mass (M), Buoyancy (F_B), Tethers Tension (T) and Stiffness (K).....	14
3.2.4 Response Amplitude Operations (RAO).....	15
3.2.5 Response Spectrum.....	16
3.2.6 TLP Response in Random Wave.....	16
3.2.7 Parametric Studies.....	17
3.3 Lab Test.....	17

CHAPTER 4 RESULT AND DISCUSSION.....21

4.1 Numerical Studies.....21

4.1.1 Energy PM and JONSWAP Spectrum Waves
Model.....21

4.1.2 Response Amplitude Operator (RAO) for PM
Spectrum.....22

4.1.3 Response Amplitude Operator (RAO) for
JONSWAP Spectrum.....23

4.1.4 Surge Response of the Triangular TLP under PM
and JONSWAP Spectrum Wave Energy.....24

4.1.5 Heave Response of the Triangular TLP under PM
and JONSWAP Spectrum WaveEnergy.....26

4.1.6 Pitch Response of the Triangular TLP under PM
and JONSWAP Spectrum Wave Energy.....27

4.2 Lab Test.....29

4.2.1 Motion Response in Surge Degree of Freedom.....29

4.2.2 Motion Response in Heave Degree of Freedom.....30

CHAPTER 5 CONCLUSION AND RECOMMENDATION.....32

CHAPTER 6 ECONOMICS BENEFITS.....34

REFERENCES.....36

APPENDICES.....38

LIST OF FIGURES

Figure 1: TLP tethers	5
Figure 2: Spar moorings	5
Figure 3: Comparison of the JONSWAP and Pierson- Moskowitz Spectra	10
Figure 4: Plan of triangular TLP.....	13
Figure 5: TLP model	18
Figure 6: Project Methodology Diagram	20
Figure 7: PM and JONSWAP spectrum model.....	22
Figure 8: RAO in Surge (PM).....	23
Figure 9: RAO in Heave (PM).....	23
Figure 10: RAO in Pitch (PM).....	23
Figure 11: RAO in Surge (JONSWAP)	24
Figure 12: RAO in Heave (JONSWAP).....	24
Figure 13: RAO in Pitch (JONSWAP).....	24
Figure 14: Surge response (PM Spectrum).....	25
Figure 15: Surge response (JONSWAP).....	25
Figure 16: Heave response (PM Spectrum).....	26
Figure 17: Heave response (JONSWAP).....	27
Figure 18: Pitch response (PM Spectrum).....	28
Figure 19: Pitch response (JONSWAP).....	28
Figure 20: TLP motion response in surge degree of freedom under influence of PM and JONSWAP spectrum model.....	30
Figure 21: TLP motion response in heave degree of freedom under influence of PM and JONSWAP spectrum model.....	31
Figure 22: Number of floating production systems units currently in operation or in order.....	34

LIST OF TABLES

Table 1: Geometric properties of the TLP.....12

Table 2: Structural Data.....12

Table 3: Environmental Data.....12

CHAPTER 1

INTRODUCTION

1.1 Background of Study

Tension Leg Platform (TLP) is a buoyant platform held in place by mooring system. TLP's are similar to conventional fixed platforms except that the platform is maintained on location through the use of moorings held in tension by the buoyancy of the hull. The mooring system is a set of tension legs or tendons attached to the platform and connected to a template or foundation on the seafloor. The template is held in place by piles driven into the seafloor. This method dampens the vertical motions of the platform, but allows for horizontal movements. The topside facilities (processing facilities, pipelines, and surface trees) of the TLP and most of the daily operations are the same as for a conventional platform.

The hull is a buoyant structure that supports the deck section of the platform and its drilling and production equipment. A typical hull has four air-filled columns supported by pontoons, similar to a semisubmersible drilling vessel. The deck for the surface facilities rests on the hull. The buoyancy of the hull exceeds the weight of the platform, requiring taut moorings or "tension legs" to secure the structure to the seafloor. The columns in the hull range up to 100 ft in diameter and up to 360 ft in height; the overall hull measurements will depend on the size of the columns and the size of the platform. [Tension Leg Platform, Global Scurity. Com]

The tether system turned out to be the major high-cost element, and one of the solutions is to change the TLP configuration into triangular shape. With a three legged structure, an equal distribution of tension naturally takes place, giving the platform a stability which is well suited to rough sea states. Compared to three columns TLP, four column TLPs are more complicated, costly and time consuming installation operation to achieve the required distribution of tension.

Until today, there is still no actual triangular tension leg platform constructed and fabricated. This type of TLPs is still under research and design phase. Research on triangular TLP has begun more popularly among professionals in deep water structure industry. As one of the countries that also moving toward the deep water technology, Malaysia also need to develop its own expertise in this related field. All studies will contribute to developing the actual triangular tension leg platform, thus adding more Malaysian professional expertise in deep water technology.

1.2 Problem Statement

Malaysia currently has moved a step forward in offshore industry by developing deep water field platform such as in Kikeh and Gemusut Kakap fields. Both are floating structures. Tension leg platform also a floating type of structure. Conventional design of TLP has 4 leg and all of this leg is connected by pretension cable call tethers to the seabed. The cost for TLP increases with the water depth. More studies to find the solution to reduce the cost by making some inovasion on TLP design. Recently, a triangular configuration type of TLPs is proposed. Many studies had been done to determine the reliability of the structures compared to the conventional 4 leg TLP.

Further studies are needed on the triangular TLP before it can be commercialized. There are many parameters need to be tested to analyze their relationship especially in Malaysian sea water environment. All parameters that will be tested, contribute to the design of the triangular TLP. Without the research, the designer can't design the triangular TLP accurately according to the environmental condition, internal and external TLP structure loads. One of the environmental elements that can affect the motion response of the platform is the wave energy. In actual sea water environment the wave energy come in various types. For now, there is no sufficient information on the behaviour of the triangular TLP in different type of wave energy spectrum.

Studies on deep water offshore structure is considered a crucial movement in oil and gas industries. Deep and continues research need to be established in order to fulfil the demand of the industry and thus create an archive of research in deep water

offshore technologies. By doing this research, it will give benefits to the related company to the industry to better understand on the deep water structure behaviour thus reduce the dependency toward the foreign consultancy. It is an aim that this practice will continue and will help to create more experts in offshore industry in the future.

1.3 Objective

At the end of the study, several objectives that expected to be achieved which are:

- Determine the dynamic response of the TLP on the surge, heave and pitch degree of freedom due to random wave.
- Determined TLP's motion response by testing a scaled down triangular TLP model in the lab.
- Determined the triangular TLP motion responses by varying the energy Spectrum due to random waves.

1.4 Project Scope and Overview

For the purpose of this study, the author will focus on the triangular tension leg platform. This study will include hydrodynamic analysis and force calculations on the structure related to the metocean data of the field under random wave. Selection of the field is based on the complete design data of the triangular TLP platform and known environment condition of the field. These parameters are important in order to design the triangular tension leg platform model for this study.

To give better understanding of the dynamics response of the triangular TLP, a numerical calculation on determined motion response had to be done. The motion response is due to random waves and as beginning, PM spectrum were used in the process. All calculation will be done using Microsoft Excel and result will be presented in graph. After completing the calculation for PM spectrum, the same calculation process will be repeated using JONSWAP spectrum. The motion response for both spectrum models will be analyzed and compared.

To achieve the objective, the scaled model will be tested in the offshore lab to observe the behaviour for both PM and JONSWAP spectrum. The analyzed data and result will be discussed to show whether the objective are achieve or not. Finally, all the work done for these studies will be documented in a proper report for future reference.

CHAPTER 2

LITERATURE REVIEW

2.1 Tension Leg Platform

A Tension Leg Platform (TLP) is floating type structure that held in place by a vertical mooring system. Different from Spar which is another type of floating structure, the mooring system in TLP is held in tension by the buoyancy of the TLP's hull. Figure 1 and 2 shows the difference of the mooring line between TLP and Spar. These mooring lines in TLP are call tethers or tendons. A set of tethers is attached and connected to a template or foundation to the seafloor. The pretension tethers condition will dampens the vertical motion of the platform, but allow for horizontal movement. (Tension Leg Platform, Global Security. Org)

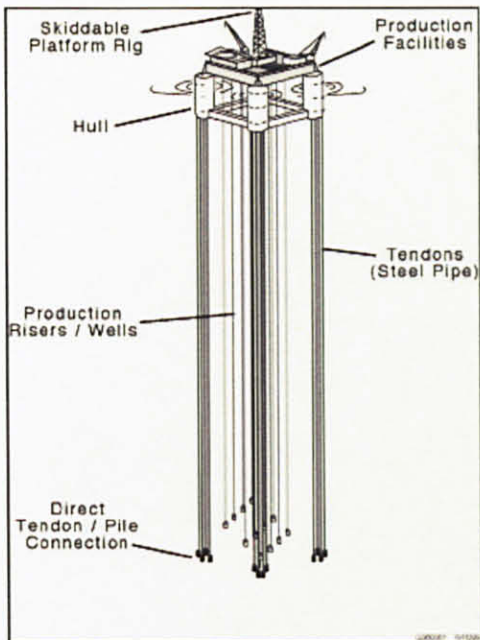


Figure 1: TLP tethers



Figure 2: Spar moorings

(Figure taken from Global Security. Org)

2.1.1 TLP Foundation

The main characteristic that differentiates TLP with other floating structures is the tethers. The tethers are connected to the template or foundation on the seafloor. The templates are strengthening with numbers of pile to ensure the platform is maintained on the location. The foundation soil of the TLP is subjected to cyclic loading continuously from ocean wave and frequently due to earthquake. According to Thomas F. Z (1990), in his journal about the effect of the frequency of cyclic loading on TLP foundation soil, the accumulated soil deformation is inversely proportional to the frequency of the applied loading. In certain cases, when comparing laboratory and field result, this could lead to an unsafe situation. Thomas F. Z founding justify of how important to carefully set up the TLP foundation to ensure stability of the platform.

2.1.2 TLP Shape and Hydrodynamic Coefficients.

Tension legged platform is a kind of offshore platform type generally used for deep water oil exploration. In future, oil explorations become more extreme by drilling wells reaching overwhelming depth which is more than 1000m. The increases in cost of fixed offshore structure with increased water depths encourage the development of compliant-type platforms. Triangular tension legged platform was propose to overcame this situation. Present TLPs have 4 hull and this hulls are attached to pretension cables called tethers that connected to seabed. Based on the triangular TLP design, there are only three legs, which mean cost for one leg can be cut off.

Chandrasekaran and Jain (2002) studied the dynamic behaviour of square and triangular offshore tension leg platform under regular wave loads. They compared the behaviour of two types of TLP which is the conventional square TLP and triangular TLP. They use the scale model to test out the behaviour. The platform is considered as a rigid body having six degree of freedom. It is concluded that, the triangular TLP exhibits a lower response in the surge and heave degrees of freedom than that of the four legged TLP considered for comparing response, under regular wave. However, the triangular TLP attracts more forces in the pitch degree of

freedom and the response in this degree of freedom is more than that of the four legged TLP. The pontoons, which are neither perpendicular nor parallel to the unidirectional wave, attract forces in the surge direction, which result in the moment about the sway axis (pitch direction). Hence, the triangular TLP, which has inclined pontoons, attract more force in the pitch and. Therefore, its responses in this degree of freedom is more than that of the four legged TLP, in which all the pontoons are either perpendicular or parallel to the unidirectional wave.

Several investigators have developed analytical and numerical tools for evaluation of forces and characteristics of different geometrical shape at different water depths of submergence. Deeper the water depth means more of the parameter need to be evaluated. Sarpakaya and Isaacson (1980) showed that C_d - C_m are functions of Keulegan-Carpenter number (K_c), Reynold number, and roughness parameter of the cylinder. The Keulegan-Carpenter number (K_c) is a measure of water particle orbital amplitude with respect to cylinder diameter, and has been defined in terms of amplitude of water particle velocity. Chandrasekaran et al. (2004) presented the influence of hydrodynamic coefficients in the response behaviour of triangular TLPs in regular waves. The variation in the coupled surge response is significant with varying C_d - C_m values when compared with that of constant coefficients. This shows that the surge response of triangular TLP is highly influenced by the values of hydrodynamic coefficients. Hydrodynamics coefficients also influence the plan dimension of TLP and its site location. Chandrasekaran et al. (2004) also stated that in all hydrodynamics cases taken for the study, it is seen that the coupled responses in all activated degrees of freedom are non linear. The variation in the response for same wave period (varying wave height) is not proportional to the variation in the response with same wave height (different wave period). Influence of hydrodynamics coefficients in the response of all activated degree of freedom is significant for the range of their variation throughout the water depth.

2.1.3 TLP Tethers

The platform is connected by the pretension cables call tethers to the seabed. This cable also influences stability of TLP. Chandrasekaran et al. (2005) investigate the stability analysis of TLP tethers. The studied was done by assuming static tension vary linearly along the tether length due to the effect of its own submerged weight. The end condition considered as simply supported and flexural rigidity of tether is neglected since it is very slender. Based on the numerical studies conducted, they concluded the tether tension variation plays an important role in the stability analysis of TLPs and its consideration is needed necessary since the water depth increases with deep water compliant structures. Lesser pretension value as shown in the 4 leg TLP leads to instability. Thus TLPs with higher initial pretension are more stable in deep water. Triangular configuration TLPs with three group tethers are more stable than the four legged TLPs in the first fundamental mode of vibration.

2.1.4 TLP Behaviour under Random Wave

The tension leg platform is a structured that behaves like a floating structure with respect to horizontal degrees of freedom, whereas with respect to the vertical degrees of freedom, it is stiff and fixed to not allow to float freely. Chandrasekaran and Jain (2001) investigate the triangular configuration tension leg platform behaviour under random sea wave loads. They shows that for orientation of the TLP and for the unidirectional wave considered, translational (surge and heave) and rotational (pitch) degree of freedom response are influenced significantly. Surge response behaviour under random waves is nonlinear since the increase in the coupled surge response is not proportional to the variation in the H_s , for the same T_z value. The response also depend on the T_z value, as the increase in the response is different when T_z changes. Variable submergence seems to be major source of non linearity and significantly enhance the response in surge, heave, pitch degrees of freedom. The variable submergence introduces tethers tension fluctuations.

2.1.5 TLP Behaviour under Impact Loading

TLPs have to safely withstand frequently occurring environmental forces arising due to wave, wind, water current and also those forces arising due to collision of ships, with icebergs or any huge sea creature. Chandrasekaran et al (2006) reported the response behaviour of triangular tension leg platforms under impact loading. They test their scale model by assuming the initial pretension in all leg is equal. Hydrodynamics constant (C_d and C_m) assumed to be constant and wave diffraction effects are neglected. The forces on the tethers are also can be neglect. Based on their numerical studies, it seen that effect of impulsive loading on triangular TLPs are significant when they act at the corner column with an inclination to the wave direction however it seen that there is no significant effect on TLP response if impulsive load act on TLP pontoons. They conclude that impulsive load, though less probable in nature, shall be considered in response analysis of deep water compliant structures as they contribute to overall dynamic stability of TLPs.

2.2 Wave Spectrum Models

Wave spectrum models are a mathematical spectrum models that are generally based or more parameters. The wave spectrum shows the distribution of energy in the wave. In 1964 Pierson and Moskowitz (1964) proposed a new formula for an energy spectrum distribution of a wind generated sea state. The PM spectrum model describes a fully developed sea determined by one parameter namely the wind speed. PM spectrum had been widely used in representing a severe storm wave in offshore structure design. The JONSWAP spectrum was developed by Hasselman, et al. (1973). JONSWAP spectrum is a five parameter spectrum, but usually three of the parameters are held constant. Ochi (1978) suggested the family of JONSWAP wave spectra in the design of an offshore structure in a fetch limited area. Figure 3 shows the comparison of the JONSWAP and Pierson- Moskowitz spectra.

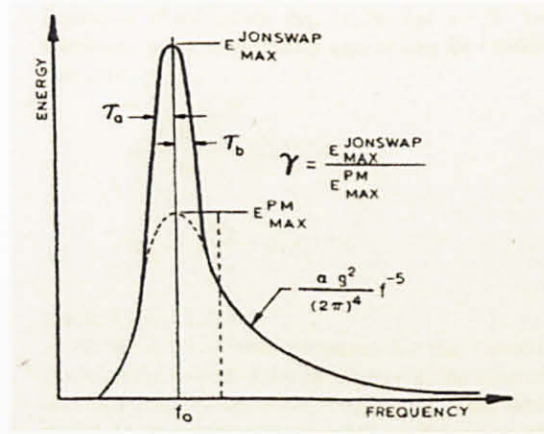


Figure 3: Comparison of the JONSWAP and Pierson- Moskowitz Spectra

Ketabdari M. J and Ranginkaman A. (2009), in their journal, simulation of random irregular sea waves for numerical and physical models using digital filters, they found out that the spectrum generated from the simulation shows desirable as realistic sea waves. Their target is to simulate three well known wave spectrum known as Pierson- Moskowitz, JONSWAP and Bretschneider spectrum. Digital filters method can be used as a powerful tool for one sided random irregular wave generation. The result also promising for generating multi directional irregular waves for 3D models by expanding model and using directional wave spectra as input.

CHAPTER 3

METHODOLOGY

Triangular TLP has major consideration for deep water application also due to its relative insensitivity with increasing water depth. This study focuses on the influence of wave energy spectrum on the motion of triangular TLP in surge, heave and pitch degree of freedom. Before setting up the model lab test, assumption and structural idealization to simplify the test had to be determined. Then a few related equation will be chosen or derive to simulate the data into graphical data. A model of triangular TLPs will be design according to the parameters that had been determined earlier. Based on the computer model, a small scale of triangular TLP model will be build for the lab test. All the behaviour or motion of the model will be captured for further analysis. The data gathered from the numerical calculation and the lab test will be analyze and discuss to conclude the analysis.

3.1 Dimensional, Structural and Environmental Data

The geometric properties of the TLP are given in Table 1. Table 2 shows the TLP structural data and Table 3 shows the environmental data for the TLP. The dimension and structural data of the triangular TLP is estimated by referring to journal from Chandrasekaran and Jain (2002). Environmental data chosen was taken from Petronas Carigali Sdn. Bhd PTS 20.073. Baram Delta environmental condition was chosen but with some adjustment to the water dept from 75 meter to 1000 meter. This adjustment had to be done to give more realistic deep water depth for TLP. Figure 4 shows the plan and the coordinate system use for the numerical studies.

Table 1: Geometric properties of the TLP

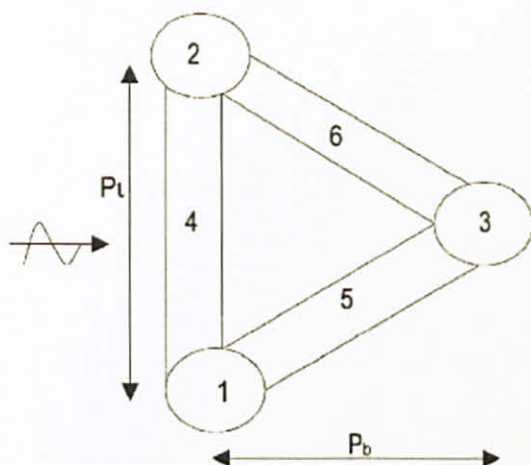
Section	Diameter (m)	Length (m)	Amount
Column	25	50	3
Pontoon	20	70	3
Tendons	1	965	12 (4 at each column)

Table 2: Structural Data

H_s (m)	3.6
T_z (s)	6.6
T_p (s)	9.3
H_{max} (m)	6.4
T_{ass} (s)	8.6
Depth (m)	1000

Table 3: Environmental Data

Total Mass (tonnes)	102000
Total Weight (kN)	1000314
Tethers Stiffness(kN/m)	10000
Draft (m)	35
Centre of Gravity (m)	7.0 (Below draft)



Point 1 = (-27.42, 975, -47.5)

Point 2 = (-27.42, 975, 47.5)

Point 3 = (54.85, 975, 0)

Figure 4: **Plan of Triangular TLP**

3.2 Numerical Studies

3.2.1 Assumptions

To establish any relationship or data analysis in the lab test, few assumptions and structural idealization must be made. This is to ensure that the lab test is in control and only the particular parameters will be tested. For this test, initial pre tension in all tethers is equal and remains unaltered over time. It is quite large in comparison to the changes that occurred during the life time of TLP. However, total pretension changes with the motion of platform. Wave forces are estimated at the instantaneous position of the platform by Morison's equation with Airy's linear wave theory. Wave is considered to act unidirectional in the surge direction only. Wave diffraction effect and wave forces on the tethers are assumed to be negligible. The low frequencies drift oscillation in surge and high frequency tension oscillation of the tethers are not considered in the analysis.

3.2.2 Force Calculation

As a basis of the research, the behaviour or relations between the parameters were needed to be familiarized. By using the environmental condition that had been chosen, all forces for surge, heave and pitch were calculated. The forces calculated

were acting on all three hulls or columns and pontoons. To calculate the resultant force due to the environmental load, Morison Equation was use.

$$F = \rho C_m A \dot{u} + \frac{1}{2} \rho C_d A u |u|$$

Where,

$$\text{Inertia Force, } F_I = \rho C_m A \dot{u}$$

$$\text{Drag Force, } F_d = \frac{1}{2} \rho C_d A u |u| \quad \text{Take } C_d = 0.65 ; C_m = 1.6$$

3.2.3 Mass (M), Buoyancy (F_B), Tethers Tension (T) and Stiffness (K).

For each of degree of freedom, the pretensions of the cable or tethers were calculated by determining the buoyancy force of the triangular TLP. The buoyancy forces deducted by the TLP weight will resultant the pretension force of the tethers. Before determined the tethers tension the mass of the structure in each degree of freedom must be calculated. To determine the mass, the TLP actual mass must be added with the structural added mass for their respective degree of freedom. The formulae involve are:

Mass

$$\text{Mass, } M = \text{Actual Mass, } M + \text{Added Mass, } M_{\text{ADD}}$$

Buoyant Force

$$F_B = (V_{\text{HULLS}} + V_{\text{PONTOONS}}) \times 1025 \times 9.807 / 1000$$

Tethers Tension

$$\text{Buoyancy, } F_B = \text{Structure weight in air, } W + \text{Tethers tension, } T$$

$$T = B - W$$

Surge Stiffness

$$K_{\text{SURGE}} = T/L$$

L = Tether length,

3.2.4 Response Amplitude Operations (RAO)

RAO for surge, heave and pitch degree of freedom can be calculate to determine the distance that the TLP responses to the forces. RAO can be determine by using the following formulae:

$$\text{RAO}_{\text{SURGE/HEAVE}} = \frac{F/\frac{H}{2}}{[(K-m\omega^2)^2 + (C\omega)^2]^{\frac{1}{2}}}$$

$$\text{RAO}_{\text{PITCH}} = \frac{M/\frac{H}{2}}{[(K-m\omega^2)^2 + (C\omega)^2]^{\frac{1}{2}}}$$

Where,	F	=	Total horizontal/vertical force
	M	=	Moment at Z-axis
	H	=	Wave height
	K	=	Surge stiffness
	C	=	Dumping with $\xi = 0.05$
	m	=	Total Mass

3.2.5 Response Spectrum

After RAO for surge and heave due to regular waves were determined, the calculation can proceed to calculate the motion response due to random waves. The calculation process begins by generating the energy spectrum model. The PM spectrum model is written as

$$S(\omega) = \alpha g^2 \omega^{-5} \exp \left[-1.25 (\omega / \omega_0)^{-4} \right]$$

Where $\alpha = 0.0081$

An equivalent expression for the PM spectrum in terms of the cyclic frequency, written as

$$S(f) = 2\pi [S(\omega)]$$

From the generated energy spectrum model, the height at a particular frequency can be calculated. At a frequency f_1 , the energy density is $S(f_1)$. The wave height at this frequency is obtained as follows

$$H(f_1) = 2\sqrt{2S(f_1)\Delta f}$$

By using respective wave height for every frequency, RAO for a particular frequency also can be calculated. The response spectrum can be obtained by multiply a square of the RAO with wave spectrum at a given frequency. Symbolically,

$$S_R(f) = [RAO(f)]^2 S(f)$$

3.2.6 TLP Response in Random Wave

For a given horizontal coordinate, x , which is the location of the triangular TLP and time, t , the wave profile is computed from

$$\eta(x, t) = \sum_{n=1}^N \frac{H(n)}{2} \cos[k(n)x - 2\pi f(n)t + \varepsilon(n)]$$

All numerical data were plotted in the graph for better analysis.

To determine the TLP motion response, RAO for respective frequency are multiply with the wave profile. The motion response for surge, heave and pitch degree of freedom are plotted in the graph.

3.2.7 Parametric Studies

The parameter that will be tested is the energy spectrum model. The spectrum models that were chosen are Pierson-Moskowitz and JONSWAP spectrum. The same calculation process that been mentioned above were used to determined the TLP response for JONSWAP spectrum model. The only difference is the spectrum generated was obtained by using the following formulae

$$S(\omega) = \alpha g^2 \omega^{-5} \exp \left[-1.25 (\omega / \omega_0)^{-4} \right] \gamma^{\exp \left[-\frac{(\omega - \omega_0)^2}{2\tau^2 \omega_0^2} \right]}$$

Where $\gamma = 3.30$

$$\tau = 0.07 \text{ if } (\omega \leq \omega_0)$$

$$= 0.09 \text{ if } (\omega_0 \leq \omega)$$

$$\alpha = 0.0081$$

3.3 Lab Test

A model of triangular TLP was design using the computer software. For this case, AutoCad software will be use to design the triangular TLP. The Triangular TLP is design using the configuration that was determined earlier. Based on the computer modal, a scale down model are build. The model will be build carefully so that it is not so much different from the actual scale triangular TLP model. The model will be use for the actual lab test. Response from three degree of freedom will be analyzed

which are surge responses, heave response and pitch response. Figure 5 shows the picture of the constructed triangular TLP model.



Figure 5: TLP model

The lab test will be done in the Offshore Structure Laboratory in Universiti Teknologi Petronas. The lab is consisting of a huge water tank and wave generator. The lab procedures are as below:

- 1) The water tank will be filling with water at the height of 1.0m.
- 2) Triangular TLP model will be float on the water.
- 3) A cable will be attached from the TLP legs to the concrete block that was submerged at the water tank bed.
- 4) The cable will be adjusted according to the draft required to make the cable in tension condition.
- 5) Wave generator will generate the PM spectrum wave.
- 6) Any motion of the triangular TLP will be observe and record.
- 7) The experiment will repeat at step 5 and 6 but this time using JANSWAP energy spectrum waves.

All the data gathered will than computed to analyze the relationship of the data. The data are simulated in the computer spreadsheet to get the graph related to the

findings. From the graph, the data will be studied to analyze any relationship and findings. Based on the result, the test can be conclude to determined whether the objectives are achieve or not.

Project methodology diagram are shown in the Figure 6. To show clearer of the project flow, the Gantt chart is provided in the *Appendix A*.

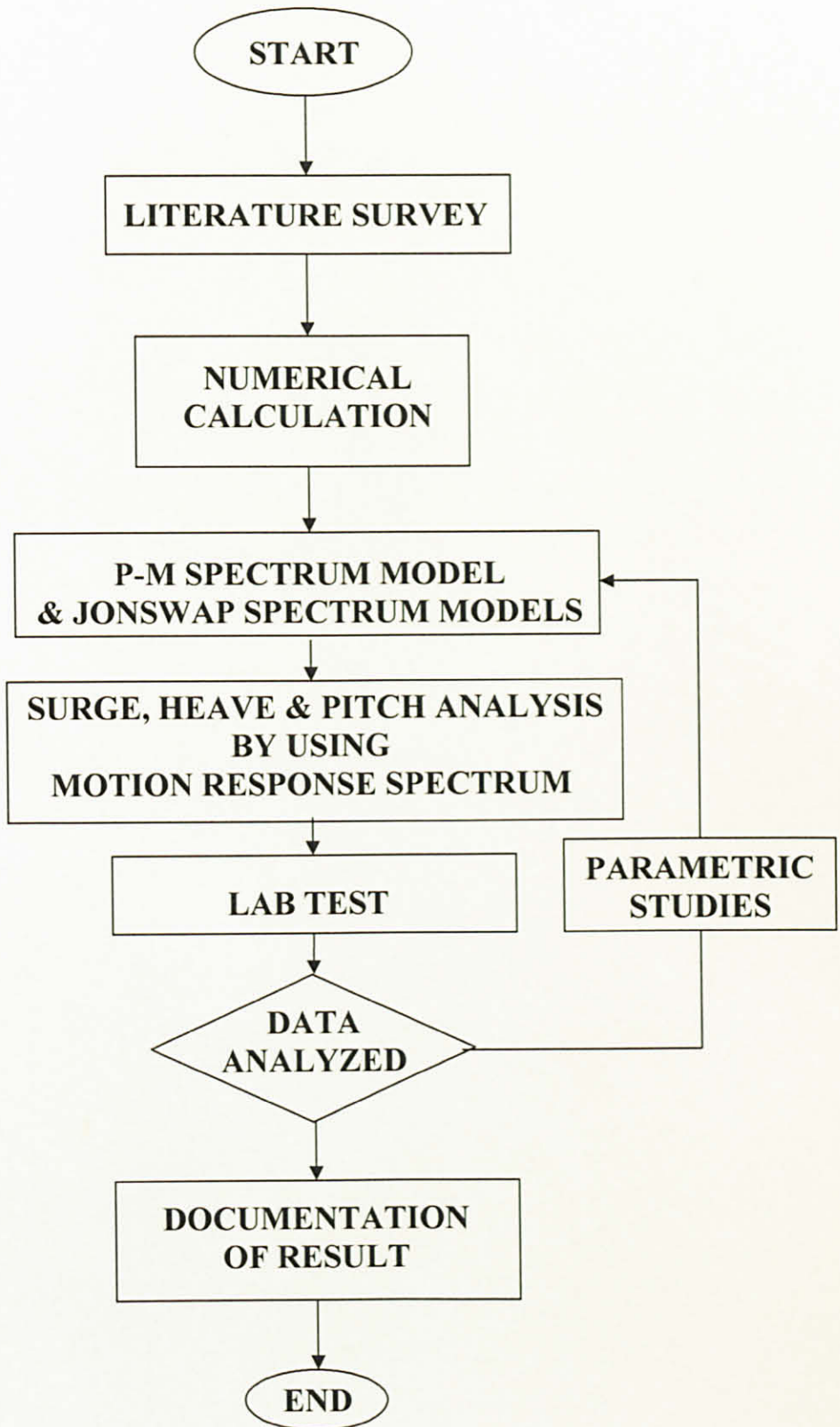


Figure 6: Project Methodology Diagram

CHAPTER 4

RESULTS AND DISCUSSIONS

Numerical studies for evaluating the motion responses of the TLP under random waves have been carried out. The TLP motion responses are compared between two type of wave energy spectrum which are Pierson-Moskowitz (PM) and JONSWAP spectrum. Wave forces are taken to be acting in the direction of surge degree of freedom. Since the wave is unidirectional, there would be no moment in the roll degree of freedom. Because of the vertical water particle velocity and acceleration, the heave degree of freedom would experience wave force. The force in the surge direction on the vertical members will cause moment in the pitch degree of freedom. However, forces in the surge degree of freedom are symmetrical about X-axis (due to the symmetry of the platform to the approaching wave) and there will be no net moment caused in the yaw degree of freedom.

4.1 Numerical Studies

4.1.1 Energy PM and JONSWAP Spectrum Waves Model.

Analysis begins by generating the Pierson-Moskowitz Spectrum (PM Spectrum) by using the given environmental and structural data. For parametric studies, the JONSWAP spectrum model also generated. The tabulated calculation is prepared at *Appendix B*. Figure 7 shown the graph of the PM and JONSWAP spectrum waves that been generated. According to the methodology, the spectrum graph will also determine the wave high for every frequency. These wave high will be use to determine the forces acting on surge, heave and pitch degree of freedom.

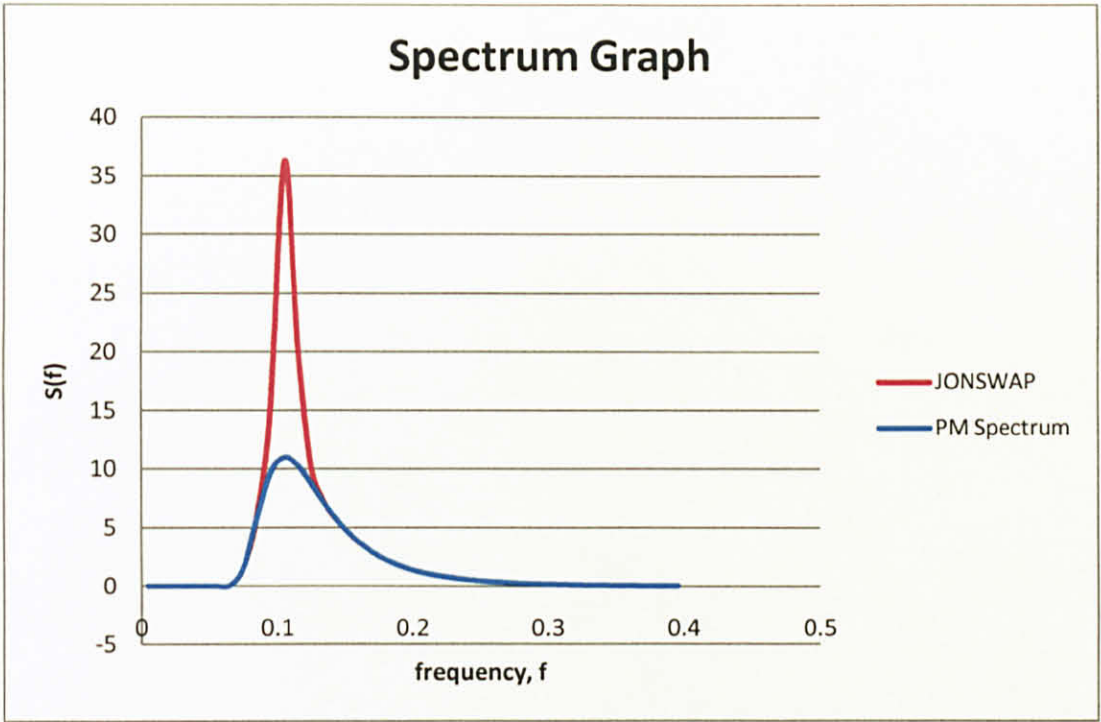


Figure 7: PM and JONSWAP spectrum model

As shown in the graph, JONSWAP spectrum had higher peak than PM spectrum. The spectrum graph shows the energy distribute by the wave. This means that, JONSWAP had higher distributive energy compared to PM spectrum. Early observation had indicated that the effects on the triangular TLP for JONSWAP spectrum model will be higher than PM spectrum. This is because the energy of the wave will determine the height of the wave. Hence, higher force acting on TLP under influence of JONSWAP spectrum model.

4.1.2 Response Amplitude Operator (RAO) for PM Spectrum

RAO for surge, heave and pitch degree of freedom were determined based on the wave height generated by the PM spectrum wave. Figure 8, 9, and 10 shows RAO for surge, heave and pitch degree of freedom. Tabulated calculation can be seen in *Appendix C*. RAO for surge is significantly higher than heave degree of freedom. In pitch degree of freedom, RAO are obtained in degree unit which is the angle of the triangular TLP corresponding to PM spectrum wave.

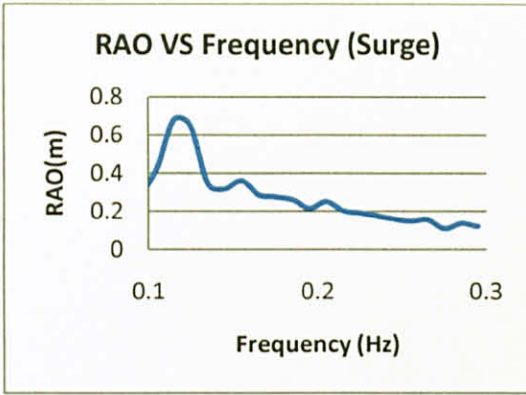


Figure 8: RAO in Surge (PM)

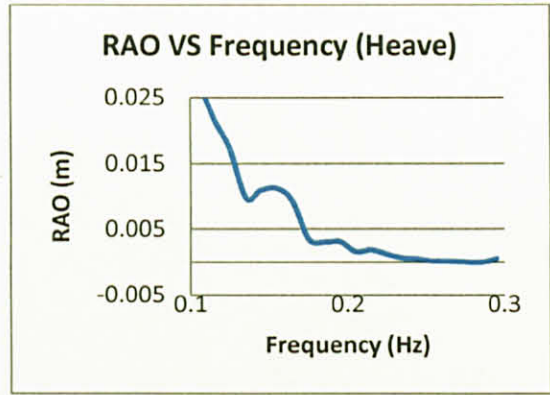


Figure 9: RAO in Heave (PM)

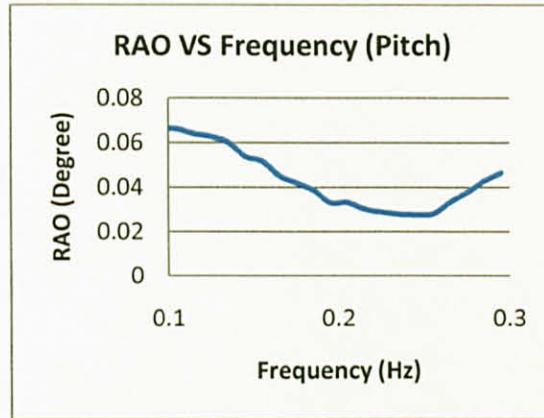


Figure 10: RAO in Pitch (PM)

4.1.3 Response Amplitude Operator (RAO) for JONSWAP Spectrum

RAO for surge, heave and pitch degree of freedom are determined based on the wave height generated by the JONSWAP spectrum wave. Figure 11, 12 and 13 shows RAO for surge heave and pitch degree of freedom. Tabulated can be seen in *Appendix D*. By comparing the RAO in JONSWAP with PM spectrum, there are no significant different in the behaviour of the graph. Only on surge degree of freedom, RAO reach the peak earlier in PM spectrum compare to JONSWAP spectrum model. RAO on surge, heave and pitch degree of freedom for PM spectrum were slightly higher than JONSWAP spectrum. This were related to the spectrum graph that been generated previously. From the spectrum graph, JONSWAP spectrum give higher peak which mean higher wave height compare to PM spectrum. The height of the wave will influence the RAO. As a result, JONSWAP spectrum had the RAO value slightly lower than PM spectrum.

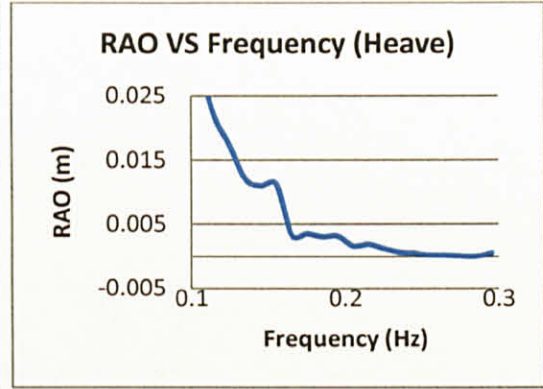
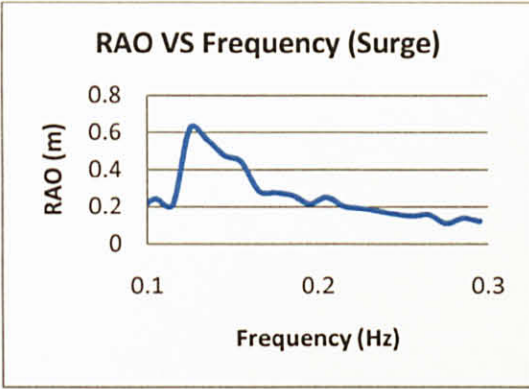


Figure 11: RAO in Surge (JONSWAP) Figure 12: RAO in Heave (JONSWAP)

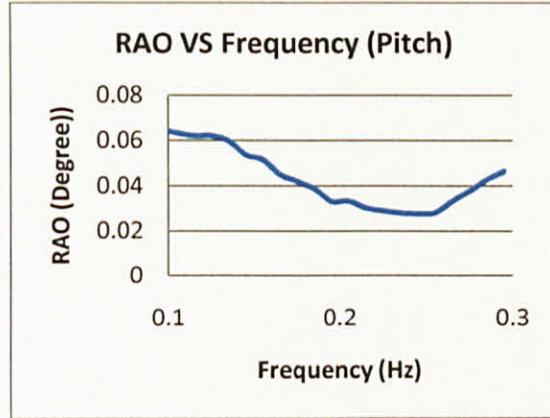


Figure 13: RAO in Pitch (JONSWAP)

4.1.4 Surge Response of the Triangular TLP under PM and JONSWAP Spectrum Wave Energy.

Figure 14 shows the motion responses on the surge degree of freedom under influence of PM spectrum wave energy. The first peak occurs at time 43s with the motion distance of -1.5m (negative sign indicate the response is in the opposite direction). The second peak occurs at time 137s with the motion distance of 1.5m. Hence, the maximum motion response in surge degree of freedom under influence of PM spectrum wave energy is 1.5m. It shows that the wave has a significant effect on the TLP.

Figure 15 shows the motion responses on the surge degree of freedom under influence of JONSWAP spectrum wave energy. Compare to the responses under PM spectrum, there are four peak motion responses in 200s time period. The maximum motion distance is a little bit shorter than in PM spectrum. The maximum distance is 1.23m. By comparing the motion responses under this two type of spectrum modal,

the difference in motion distance is not significant with just only 0.47m difference but the motion frequency of the TLP is more vigorous under influence of JONSWAP spectrum energy wave. Tabulated calculation is attached in *Appendix E*.

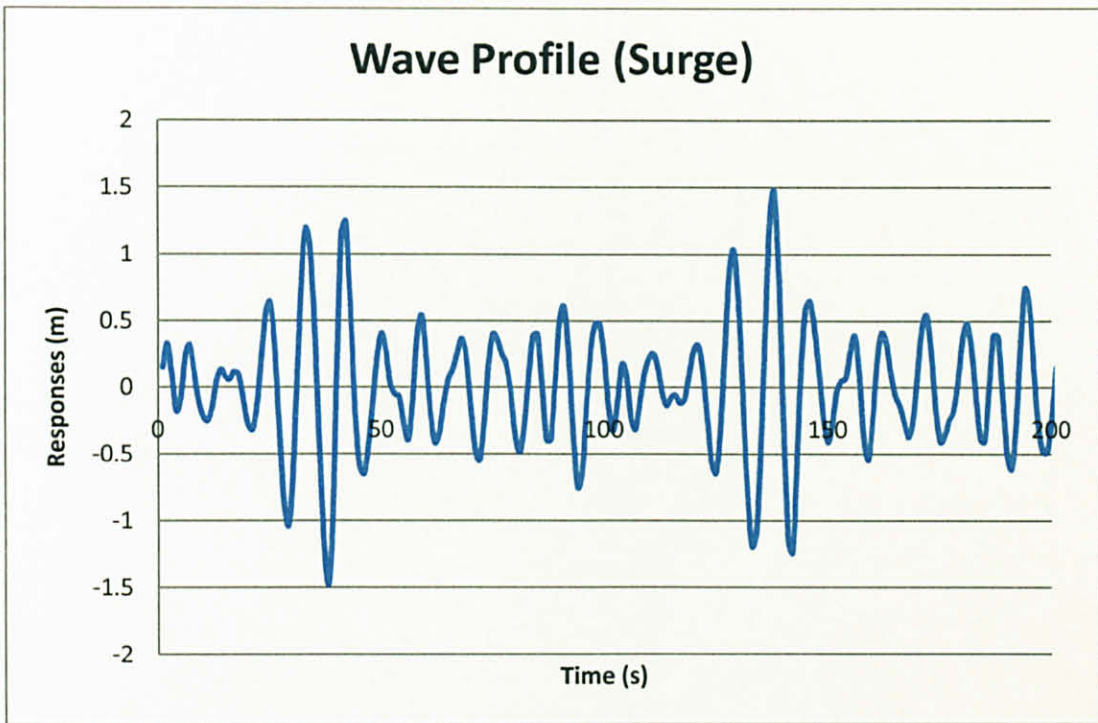


Figure 14: Surge response (PM Spectrum)

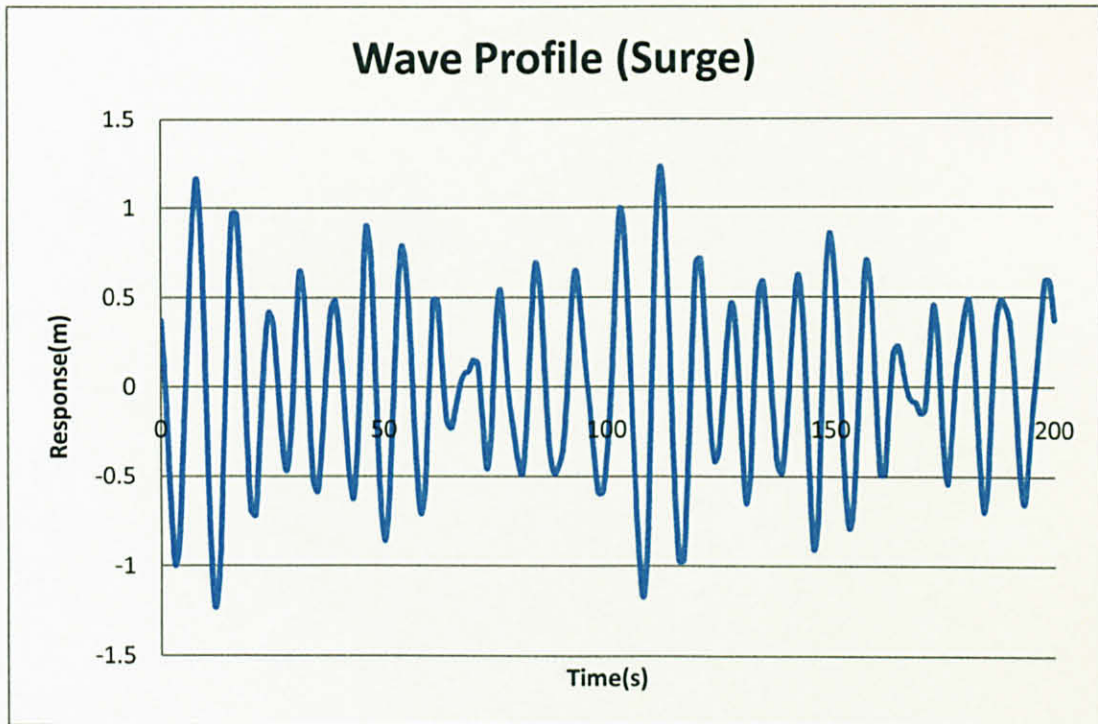


Figure 15: Surge response (JONSWAP)

4.1.5 Heave Response of the Triangular TLP under PM and JONSWAP Spectrum Wave Energy.

Figure 16 shows the motion response on the heave degree of freedom under influence of PM spectrum wave energy. It is seen that the maximum motion distance in heave degree of freedom occurs at time 37s and 137s. The maximum motion distance is 0.07m. Effect on the TLP motion response in heave degree of freedom is coming from the pressures that produce by the wave at the bottom of the TLP hull. However, the motion on heave degree of freedom is limit by the tethers pretension. That is why the motion distance on heave degree of freedom is quite low compare to surge degree of freedom.

Maximum motion distance under the influence of JONSWAP spectrum energy wave is 0.10m. This constraint in maximum motion distance occurs because of same tethers pretension magnitude use for both cases. Similar to the analysis in surge degree of freedom, the motion response in JONSWAP spectrum wave is more vigorous toward the peak compare to PM spectrum wave. Figure 17 shows the motion response on the heave degree of freedom under the influence of JONSWAP spectrum energy wave. Tabulated calculation is attached in *Appendix F*.

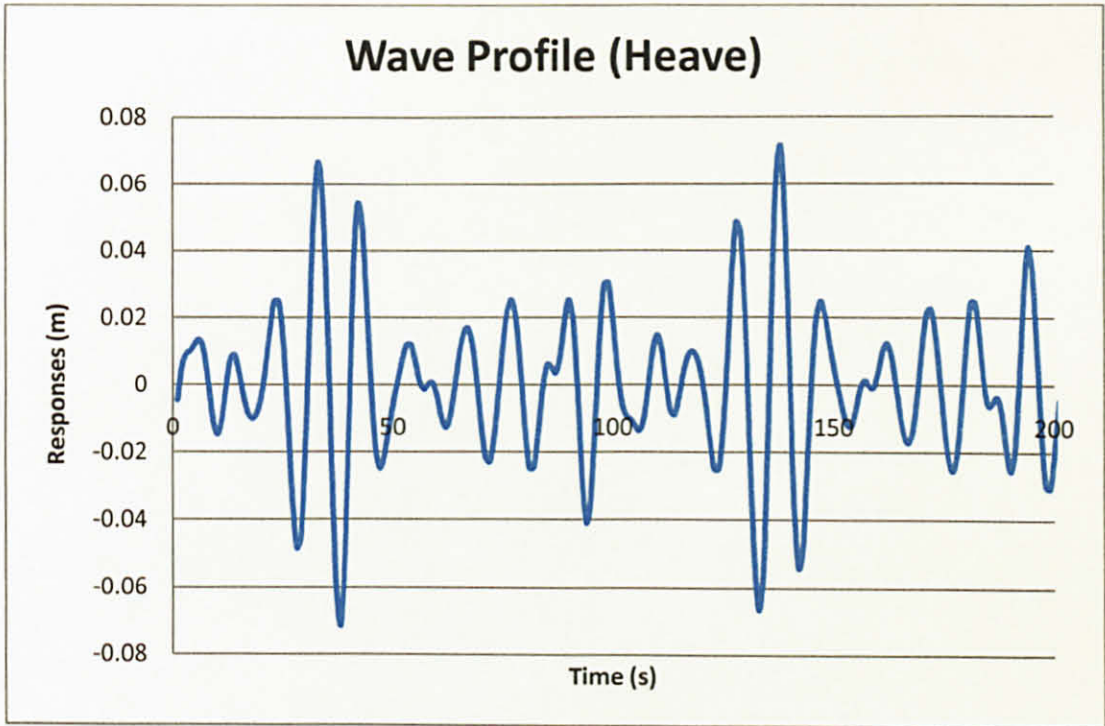


Figure 16: Heave response (PM Spectrum)

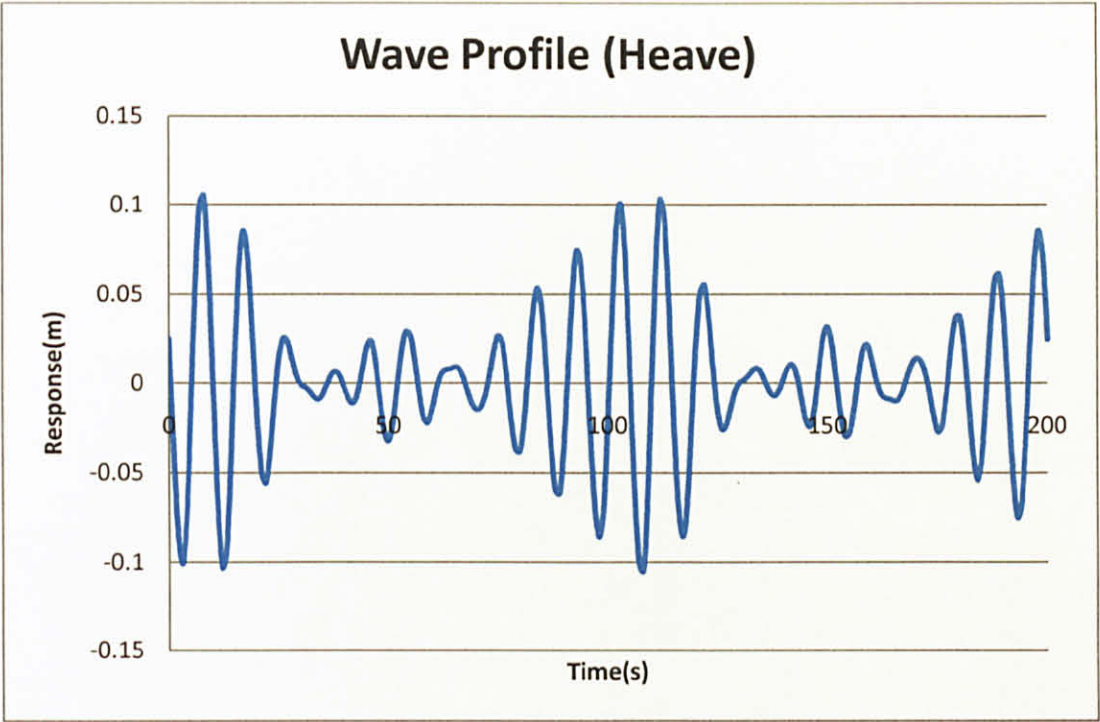


Figure 17: Heave response (JONSWAP)

4.1.6 Pitch Response of the Triangular TLP under PM and JONSWAP Spectrum Wave Energy.

Figure 18 shows the motion response on the pitch degree of freedom under influence of PM spectrum energy wave. Different from the surge and heave degree of freedom, in pitch degree of freedom, the motion is due to the resultant moment at Z-axis. The motion are seen in the TLP angle not the distance like seen in the surge and heave degree of freedom. The maximum motion angle occurs at time 37s and 137s with the angle of 0.21° .

Figure 19 shows the motion response on the pitch degree of freedom under influence of JONSWAP spectrum energy wave. Slightly higher maximum angle are produce which is 0.25° . The motion response are more vigorous toward the peak of the maximum response compare to influence of PM spectrum energy wave. These results are related to the TLP tethers which also limit the motion on the pitch degree of freedom. Similar to the motion in heave degree of freedom, the pretension of the tethers determine the limitation of the motion in the pitch degree of freedom. This is

because, the same tethers pretension values were used for both energy spectrum wave. Tabulated calculation is attached in *Appendix G*.

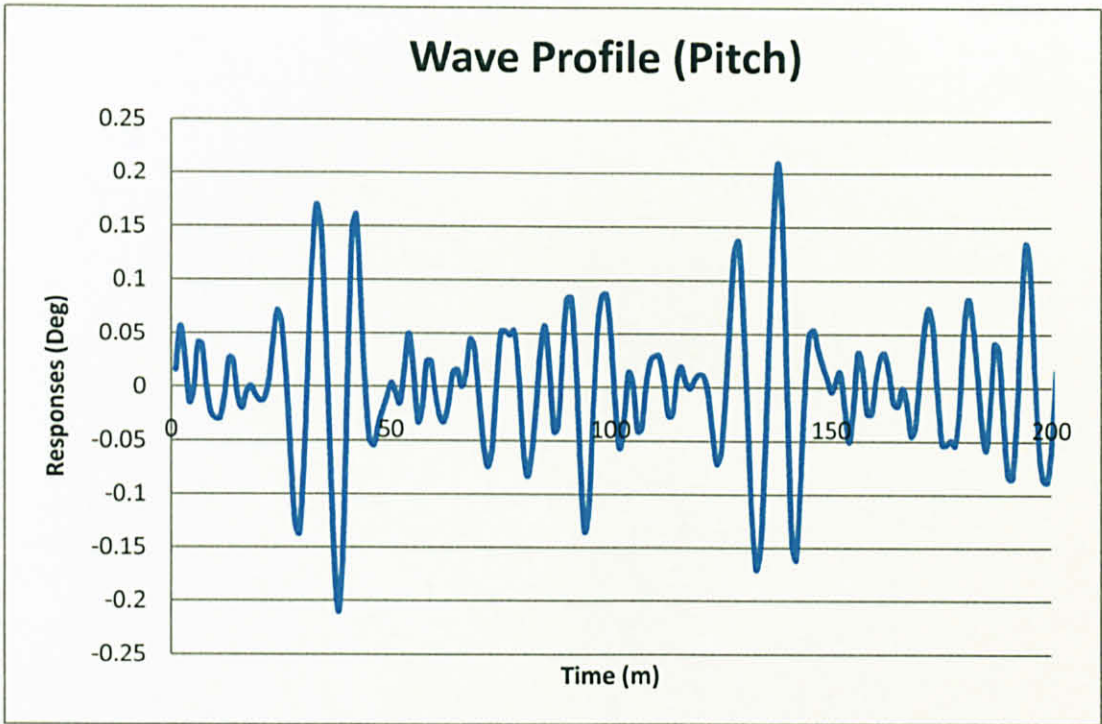


Figure 18: Pitch response (PM Spectrum)

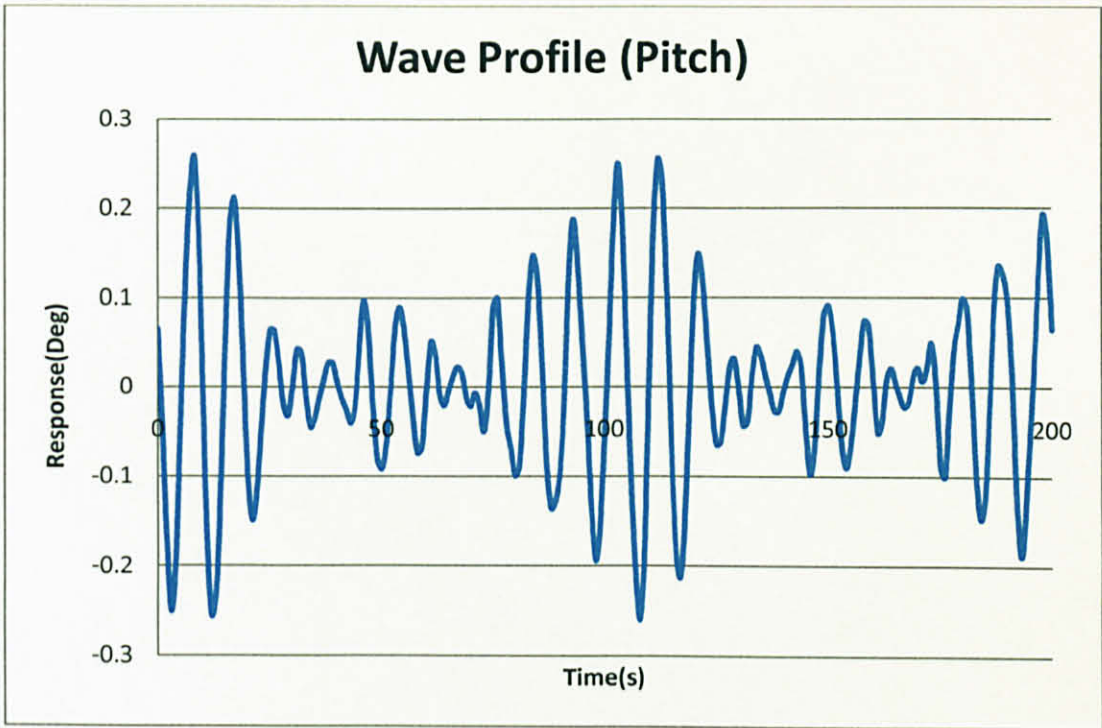


Figure 19: Pitch response (JONSWAP)

4.2 Lab Test

Lab test had been done to give more understanding on the triangular TLP motion response due to random waves. This lab test was purposely to support the numerical calculation data of the TLP motion response. The behaviour or the motion response are recorded and plotted in the graph to give clearer view. Unfortunately, motion response on pitch degree of freedom difficult to be plotted because of the motion is too small to observe and measured.

4.2.1 Motion Response in Surge Degree of Freedom

Figure 20 shows the motion response in surge degree of freedom under influence of PM and JONSWAP spectrum. The platform motion responses were recorded in 1 minute for each spectrum. By comparing the motion response for both energy spectrum modes, the motion in JONSWAP energy spectrum is more vigorous. These can be seen in the graph that in 1 minute period, the platform motion reaches the peak more often compare to motion response in PM spectrum wave. These observations justify the numerical calculation result, where the motion response for JONSWAP spectrum model in surge degree of freedom is more vigorous, but the maximum motion distance is slightly the same.

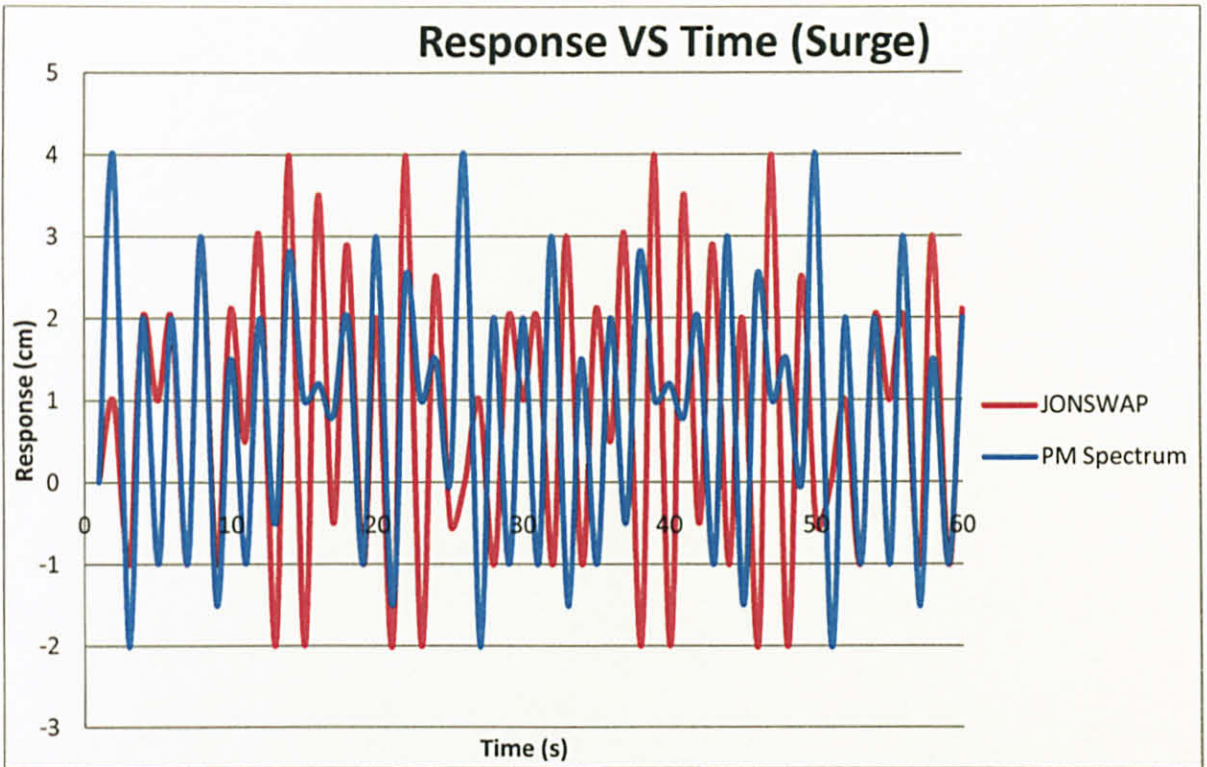


Figure 20: TLP motion response in surge degree of freedom under influence of PM and JONSWAP spectrum model.

4.2.2 Motion Response in Heave Degree of Freedom

Figure 21 shows the motion response in heave degree of freedom under influence of PM and JONSWAP spectrum. Based on the Figure 21, the motion response in heave degree of freedom is very small compare to motion response in surge degree of freedom. Similar to the result on surge degree of freedom, the motion response for JONSWAP spectrum is more vigorous compare to PM spectrum. Under influence of PM spectrum wave, the time period for the TLP to reach maximum motion is longer compare to JONSWAP spectrum wave. This resulted from the energy distribution for PM spectrum model that had lower peak compare to JONSWAP spectrum wave. Based on the lab test result, it is justify the numerical calculation on the TLP motion response in heave degree of freedom. The motion in JANSWAP spectrum is more vigorous than in PM spectrum and the maximum motion is about the same for both energy spectrum models.

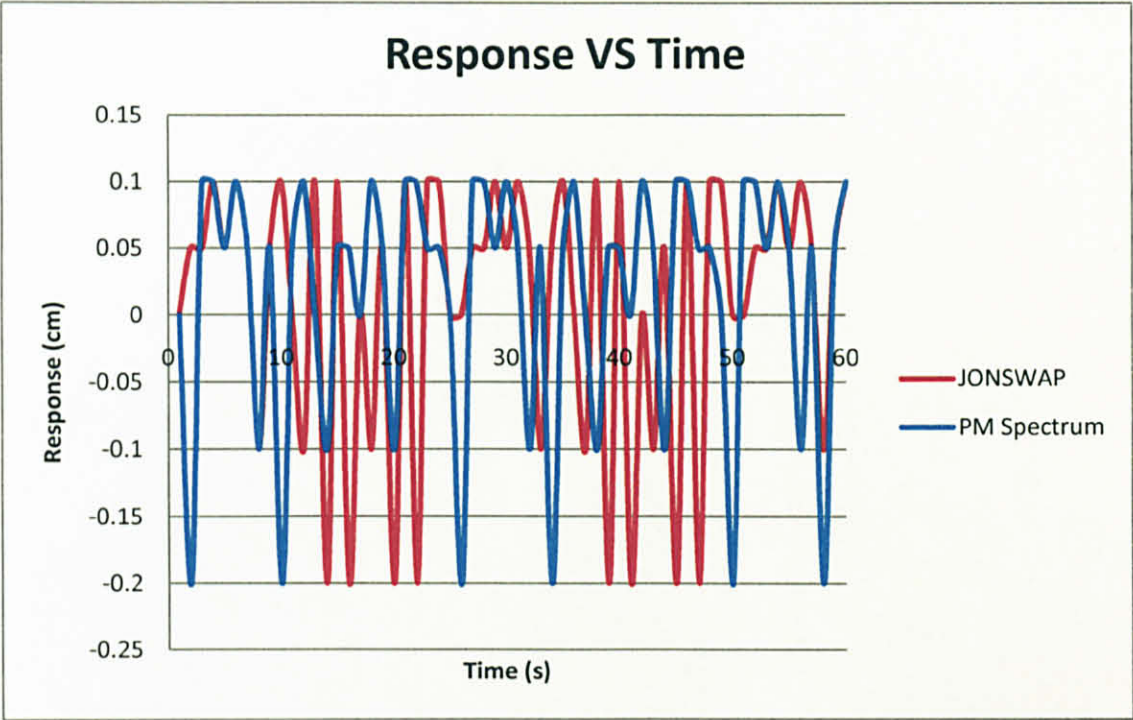


Figure 21: TLP motion response in heave degree of freedom under influence of PM and JONSWAP spectrum model.

CHAPTER 5

CONCLUSION AND RECOMMENDATION

5.1 Conclusion

Wave spectrum energy plays a significant role in the TLP motion response. The significant difference is not on the maximum motion response distance but on the frequencies of the TLP motion responses. For every degree of freedom, the motion responses under JONSWAP spectrum give more movement or higher frequencies compared to motion responses under PM spectrum. This significant difference is because of the wave energy distribution for JONSWAP spectrum is higher than PM spectrum.

After completing the numerical calculation, the motion responses for the triangular TLP can be determined in surge, heave and pitch degree of freedom. For the orientation of the TLP and for the unidirectional wave considered, translational (surge and heave) and rotational (pitch) degree of freedom responses are influenced significantly. These were happened for both PM and JONSWAP energy spectrum. Only a small significant difference in surge, heave and pitch motion response for both PM and JONSWAP energy spectrums, but the frequencies of the TLP motion on surge, heave and pitch degree of freedom can affect the TLP tethers.

A scale down model of the triangular TLP had successfully been constructed and tested. The result shows that the triangular TLP motion response under influence JONSWAP spectrum wave were more vigorous compared to motion response in PM spectrum wave. This result justifies the motion response obtained from the numerical calculation data.

TLP's motion is restricted by the tethers pretension. Every movement of the platform away from the initial location will force the tethers to pull back the platform back to

the initial location. These pulling actions were repeated for every degree of freedom and move in a certain frequency. Based on the result, the main difference between PM and JONSWAP spectrum is the frequency of the TLP motion not the maximum motion distance. This TLP motion frequency will directly influenced the tethers movement as well. There is a concern that if the platform moves in the same frequency as the tethers natural frequency, resonance effect will occur and give a big impact to the platform itself.

At this point of studies, the effect of the wave spectrum on the triangular TLP can be determined. As a designer, to design a triangular TLP, they need to select the appropriate spectrum model to analyze their TLP design. Difference sea state will give different type of wave spectrum. Wave spectrum model can effect on designing the tethers pretension and TLP dimension to give stability in a particular sea environment.

5.2 Recommendation

Based on the result, energy spectrum wave had a significant influence in how the TLP move. In other word, the motion response of the triangular TLP are move in different frequency for different energy spectrum model. In future, it is recommended to analyze the resonance effects of the TLP tethers due to the energy spectrums.

Further studies need to be done to confirm and justify that the tethers can be affected by the wave spectrum. The movements of the tethers, especially the frequencies of the motion response need to be analyze whether it can move in the same as tethers natural frequencies.

CHAPTER 6

ECONOMICS BENEFITS

Floating production has evolved to an important technology that opens for development oil and gas reservoirs that would be otherwise impossible or uneconomic to explore. The technology enables production far beyond the limited depth constraints of fixed platforms, generally considered to be 1,400 feet, and provides a flexible solution for developing short-lived fields with marginal reserves and fields in remote locations where installation of a fixed facility would be difficult.

In a report prepared by James R. McCaul (2003), President of International Maritime Associate Inc., there are four type of floating production systems that were vastly operated now. Figure 22 shows the numbers of unit of floating production systems that still operated or in order. The figure shows that TLP is less preferable type of floating production system compare to semi-sub and FPSO. Full size TLPs have fallen out of favor due to their high cost.

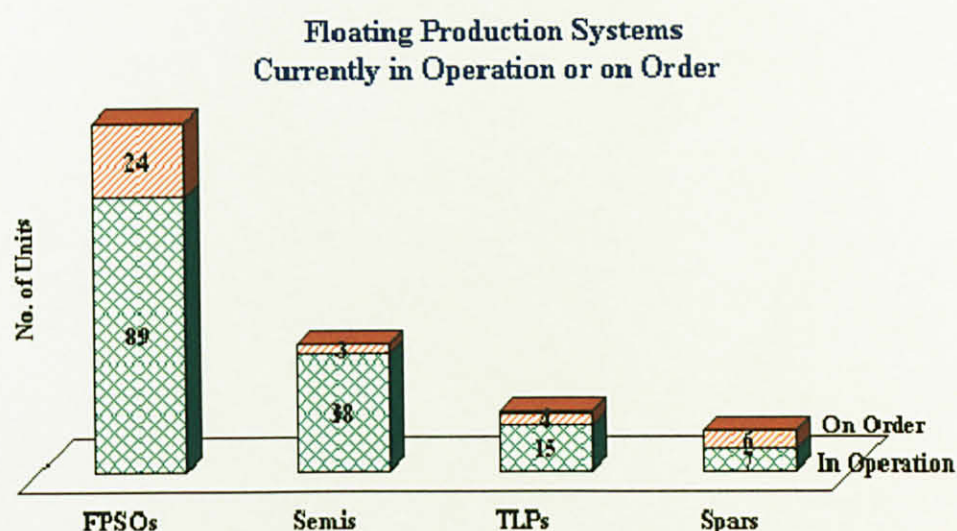


Figure 22: Number of floating production systems units currently in operation or in order

Now interest has shifted to mini-TLPs designed, Sea Star TLP and new develop triangular TLP. As been mentioning before, the conventional type of TLP is high in cost compare to semi-sub and FPSO. Conventional TLP is designed with four leg and it is cost about 650 million USD for the whole TLP. It is estimated that the cost for each leg is about 100 million USD. In addition, this cost will increase with the length of the tethers.

The new develop triangular configuration TLP had been seen can solve this problem. Triangular TLP only use three legs compare to conventional TLP which use four legs. It is simply can excluded the cost for one leg in the whole total cost of the TLP. Previously, it is estimated that the cost for each leg is 100 million USD, so the total cost for the whole triangular TLP is about 550 million USD.

This thesis is done purposely to support the effectiveness of triangular TLP. Hopefully, this thesis also can convince the oil and gas operator to invest more on development of triangular TLP which is proof to be more economical than conventional TLP. In the future, it is expected that more TLP will be construct and operate if the actual triangular TLP is proven to be economical and reliable design. For that reason, more research had to be done to show and justify the effectiveness of triangular TLP.

Besides, this research may come in handy for local oil and gas operator to explore in deep water technology without depending on foreign consultation. It is well known that foreign consultant charge higher rate for their consultation compare to local consultant. More research or studies had been done by local students means more expertise in deep water technology in the future. This development of deep water technology research will give benefits to local oil and gas operator's economy in the future.

REFERENCES

1. Chakrabarti, S.K., (2001). Hydrodynamics of Offshore Structures, Illinois, USA: WIT Press
2. Chandrasekaran S., Jain A.K, Chandak N.R, 2004. Influence of hydrodynamics coefficient in the response behaviour of triangular tension leg platform in regular waves. Journal of Ocean Engineering, Technical Note vol. 31, 2319-2342.
3. Chandrasekaran S., Jain A.K, (2002). Dynamic behaviour of square and triangular TLPs under regular waves. Journal of Ocean Engineering 29 (3), 279-315.
4. Chandrasekaran S., Jain A.K, (2001). Triangular configuration tension leg platform behaviour under random sea wave loads. Journal of Ocean Engineering 29 (3), 1895-1928.
5. Chandrasekaran S., Chandak N.R, Gupta Anupam, (2005). Stability analysis of TLP tethers . Journal of Ocean Engineering 33. 471-482.
6. Chandrasekaran S., Jain A.K., Gupta A., Srivastava A., (2006). Response behaviour of triangular tension leg platform under impact loading. Journal of Ocean Engineering 34. 45-53.
7. James R. McCaul, (2003). Outlook for floating production systems, International Maritime Associates. Inc.
8. Ketabdari M. J, Ranginkaman A. (2009). Simulation of random irregular sea waves for numerical and physical models using digital filters. Transaction B: Mechanical Engineering (pp 240 – 247), Sharif University of Technology.

9. Sarpakaya T., Isaacson M., (1981). Mechanics of wave forces on offshore structure. London, Van Nostrand Reinhold Co.
10. Tension leg platform. Global Security. Org.
<https://www.globalsecurity.org/military/systems/ship/platform-tensionleg.htm>.
11. Thomas F. Zimmie, (1990). The effect of the frequency of cyclic loading on TLP foundation soils. Journal of The International Society of Offshore and Polar Engineer.
12. PTS 20.073. (2005). Design of fixed offshore structures. Petronas Carigali Sdn. Bhd.

APPENDICES

APPENDIX A

Gantt Chart

FYP I

No.	Detail	1	2	3	4	5	6	7	8	9	10	11	12	13	14	15	16	30-nov to 3-dec	7-18 Dec	21-31 Dec
1	Selection of Project Topic																			
2	Preliminary Research Work																			
3	Submission of Progress Report																			
4	Project work continues																			
5	Submission of Interim Report Final Draft																			
6	Oral Presentation																			
7	Modal Design																			
6	Lab Testting																			
7	FYP SEMINAR 1 (EIM TALK)				12-Aug															
8	FYP WORKSHOP 1 (IRC)					17-Aug														
9	FYP WORKSHOP 2 (TECHNICAL WRITING)					17-Aug														
10	FYP WORKSHOP 3 (LAB BRIEFING)						24-Aug													
10	FYP WORKSHOP 4 (REFERENCING)									14-Sep										
10	FYP WORKSHOP 5 (HSE BRIEFING)														19-Oct					

	MILESTONE OF FYP 1
	SEMINAR / WORKSHOP

FYP II

[illegible]

APPENDIX B
ENERGY SPECTRUM MODEL
CALCULATION

PM SPECTRUM

Hass	3.6
d	1000
TP	9.3
t	0
ω_0	0.66225
g	9.80665
α	0.0081

f	ω	$\exp(-1.25(\omega/\omega_0)^4)$	$\alpha g^2 \omega^5$	S(ω)	S(f)	H(f)
0.005	0.031416	0	25455228.89	0	0	0
0.015	0.094248	0	104754.0284	0	0	0
0.025	0.15708	3.0527E-172	8145.673246	2.4866E-168	1.5624E-167	1.11799E-84
0.035	0.219911	2.25504E-45	1514.561129	3.4154E-42	2.14596E-41	1.31025E-21
0.045	0.282743	4.58641E-17	431.0865365	1.97714E-14	1.24227E-13	9.96905E-08
0.055	0.345575	4.76755E-08	158.056944	7.53545E-06	4.73466E-05	0.001946209
0.065	0.408407	0.000176495	68.55833235	0.012100204	0.076027821	0.077988626
0.075	0.471239	0.007630042	33.52128908	0.255768835	1.607042986	0.358557441
0.085	0.534071	0.052062556	17.92802296	0.933378697	5.864591314	0.684957886
0.095	0.596903	0.150465943	10.28037606	1.546846476	9.719123049	0.881776527
0.105	0.659734	0.281063456	6.232761847	1.751801585	11.00689398	0.938377066
0.115	0.722566	0.413938458	3.954921124	1.637093953	10.28616467	0.907134595
0.125	0.785398	0.531588391	2.606615439	1.385646507	8.706273772	0.834566895
0.135	0.84823	0.628477583	1.774018669	1.114930965	7.005317855	0.748615675
0.145	0.911062	0.705403784	1.241043537	0.875436807	5.500531681	0.663357019
0.155	0.973894	0.765465597	0.889136702	0.680603557	4.276358267	0.584900557
0.165	1.036726	0.812098273	0.650440099	0.528221281	3.318912192	0.515279512
0.175	1.099557	0.848330434	0.484659561	0.411151456	2.583340788	0.454606713
0.185	1.162389	0.876602354	0.367086477	0.32178887	2.021859101	0.40217997
0.195	1.225221	0.89880062	0.282133055	0.253581365	1.593298705	0.357020863
0.205	1.288053	0.916356262	0.219713996	0.201336296	1.265033258	0.318123656
0.215	1.350885	0.930346725	0.173154877	0.161094073	1.012183912	0.284560561
0.225	1.413717	0.941582454	0.137947692	0.129889126	0.816117448	0.255517897
0.235	1.476549	0.95067473	0.110990988	0.105516327	0.662978639	0.230300437
0.245	1.53938	0.958086886	0.0901149	0.086337904	0.542477051	0.20832226
0.255	1.602212	0.964172267	0.073777872	0.071134578	0.446951738	0.189092937
0.265	1.665044	0.969202175	0.060869209	0.05899457	0.370673814	0.172203093
0.275	1.727876	0.973386397	0.050578222	0.049232153	0.309334743	0.157311091
0.285	1.790708	0.976888318	0.042306074	0.04132831	0.259673429	0.144131448
0.295	1.85354	0.979836088	0.035605488	0.034887543	0.219204895	0.132425041
0.305	1.916372	0.98233092	0.03013893	0.029606403	0.186022516	0.121990989
0.315	1.979203	0.984453293	0.025649226	0.025250465	0.158653349	0.112659966
0.325	2.042035	0.986267613	0.021938666	0.021637396	0.135951769	0.104288741
0.335	2.104867	0.987825748	0.018853978	0.018624445	0.117020838	0.096755708
0.345	2.167699	0.989169717	0.016275396	0.016099128	0.101153807	0.089957237
0.355	2.230531	0.990333757	0.014108644	0.013972266	0.087790337	0.083804695
0.365	2.293363	0.991345915	0.012278992	0.012172728	0.076483507	0.078221996
0.375	2.356194	0.99222929	0.010726813	0.010643458	0.066874816	0.073143594
0.385	2.419026	0.993003	0.009404233	0.009338432	0.058675096	0.068512829
0.395	2.481858	0.993682941	0.008272591	0.008220333	0.051649872	0.064280555

JONSWAP SPECTRUM

Hass	3.6
d	1000
Tp	9.3
γ	3.3
t	0
ω ₀	0.66225
τ	0.07
g	9.80665
α	0.0081

0.09

f	ω	$\exp(-1.25(\omega/\omega_0)^4)$	$\exp(-((\omega-\omega_0)^2/(2\tau^2\omega_0^2))$	S(ω)	S(f)	H(f)
0.005	0.031416	0	1	0	0	0
0.015	0.094248	0	1	0	0	0
0.025	0.15708	3.0527E-172	1	2.4866E-168	1.5624E-167	1.11799E-84
0.035	0.219911	2.25504E-45	1	3.4154E-42	2.14596E-41	1.31025E-21
0.045	0.282743	4.58641E-17	1	1.97714E-14	1.24227E-13	9.96905E-08
0.055	0.345575	4.76755E-08	1	7.53545E-06	4.73466E-05	0.001946209
0.065	0.408407	0.000176495	1.000000368	0.012100208	0.076027849	0.07798864
0.075	0.471239	0.007630042	1.000245686	0.255831674	1.607437813	0.358601485
0.085	0.534071	0.052062556	1.026454355	0.958070629	6.019735297	0.693958806
0.095	0.596903	0.150465943	1.555914967	2.406761583	15.12212902	1.099895596
0.105	0.659734	0.281063456	3.294208207	5.770799157	36.25900048	1.703150034
0.115	0.722566	0.413938458	2.045167348	3.348131098	21.03692812	1.297287266
0.125	0.785398	0.531588391	1.151707312	1.595859214	10.02707917	0.895637389
0.135	0.84823	0.628477583	1.00921967	1.12521026	7.069904573	0.752058752
0.145	0.911062	0.705403784	1.000196282	0.875608639	5.501611334	0.663422118
0.155	0.973894	0.765465597	1.000001381	0.680604497	4.276364174	0.584900961
0.165	1.036726	0.812098273	1.000000003	0.528221283	3.318912202	0.515279513
0.175	1.099557	0.848330434	1	0.411151456	2.583340788	0.454606713
0.185	1.162389	0.876602354	1	0.32178887	2.021859101	0.40217997
0.195	1.225221	0.89880062	1	0.253581365	1.593298705	0.357020863
0.205	1.288053	0.916356262	1	0.201336296	1.265033258	0.318123656
0.215	1.350885	0.930346725	1	0.161094073	1.012183912	0.284560561
0.225	1.413717	0.941582454	1	0.129889126	0.816117448	0.255517897
0.235	1.476549	0.95067473	1	0.105516327	0.662978639	0.230300437
0.245	1.53938	0.958086886	1	0.086337904	0.542477051	0.20832226
0.255	1.602212	0.964172267	1	0.071134578	0.446951738	0.189092937
0.265	1.665044	0.969202175	1	0.05899457	0.370673814	0.172203093
0.275	1.727876	0.973386397	1	0.049232153	0.309334743	0.157311091
0.285	1.790708	0.976888318	1	0.04132831	0.259673429	0.144131448
0.295	1.85354	0.979836088	1	0.034887543	0.219204895	0.132425041
0.305	1.916372	0.98233092	1	0.029606403	0.186022516	0.121990989
0.315	1.979203	0.984453293	1	0.025250465	0.158653349	0.112659966
0.325	2.042035	0.986267613	1	0.021637396	0.135951769	0.104288741
0.335	2.104867	0.987825748	1	0.018624445	0.117020838	0.096755708
0.345	2.167699	0.989169717	1	0.016099128	0.101153807	0.089957237
0.355	2.230531	0.990333757	1	0.013972266	0.087790337	0.083804695
0.365	2.293363	0.991345915	1	0.012172728	0.076483507	0.078221996
0.375	2.356194	0.99222929	1	0.010643458	0.066874816	0.073143594
0.385	2.419026	0.993003	1	0.009338432	0.058675096	0.068512829
0.395	2.481858	0.993682941	1	0.008220333	0.051649872	0.064280555

APPENDIX C
RESPONSE AMPLITUDE OPERATOR (RAO)
FOR PM SPECTRUM

RAO (surge)	K=			M=			C=		
	0.025	0.035	0.045	0.055	0.065	0.075	0.085	0.095	0.105
H	1.11799E-84	1.31025E-21	9.96905E-08	0.001946209	0.077988626	0.358557441	0.684957886	0.881776527	0.938377066
ω	0.157079633	0.219911486	0.282743339	0.345575192	0.408407045	0.471238898	0.534070751	0.596902604	0.659734457

F.HULL 1	407342.4957	407342.4957	407342.7238	413655.0932	736722.3279	2313505.649	4714928.033	6860203.594	8035404.148
F.HULL 2	407342.4957	407342.4957	407342.7238	413655.0932	736722.3279	2313505.649	4714928.033	6860203.594	8035404.148
F.HULL 3	407342.4957	407342.4957	407342.7226	413631.9851	741992.1494	2307563.943	4793003.419	6850946.987	8023566.792
PNT00N4	-1.78141E-78	-3.788E-15	0.441627081	11577.69196	-577637.9184	-3072994.181	-6377101.519	-8609745.676	-9146874.185
PNT00N5	-4.45385E-79	-9.10517E-17	-0.011456258	-2788.336635	132391.3236	-657821.6837	-1220056.46	-1410422.78	1174332.342
PNT00N6	-4.45385E-79	-9.10517E-17	-0.011456258	-2788.336635	132391.3236	-657821.6837	-1220056.46	-1410422.78	1174332.342
TOTAL	1222027.487	1222027.487	1222028.589	1246943.19	1902581.534	2545937.694	5405645.046	9140762.939	17296165.59
F/(H/2)	2.18611E+90	1.86533E+27	2.45165E+13	1281407244	48791256.93	14201003.24	15783875.65	20732606.64	36863998.94
$(K-M\omega^2)^2$	2.2516E+13	8.98786E+13	2.49457E+14	5.61046E+14	1.09939E+15	1.95419E+15	3.23007E+15	5.04664E+15	7.53843E+15
$(C\omega)^2$	9250317683	18130622659	29971029294	44771537587	62532147539	83252859150	1.06934E+11	1.33575E+11	1.63176E+11
RAO	4.60615E+83	1.96736E+20	1552150.561	54.09665948	1.471476793	0.321237918	0.27771565	0.29184145	0.424577764

0.115	0.125	0.135	0.145	0.155	0.165	0.175	0.185	0.195	0.205
0.907134595	0.834566895	0.748615675	0.663357019	0.584900557	0.515279512	0.454606713	0.40217997	0.357020863	0.318123656
0.72256631	0.785398163	0.848230016	0.91106187	0.973893723	1.036725576	1.099557429	1.162389282	1.225221135	1.288052988

MAXIMUM TOTAL FORCE

8190290.4	8525615.896	8098495.8	7247100.73	6962941.847	6004773.037	5628269.372	5115711.55	4157093.959	4277782.634
8190290.4	8525615.896	8098495.8	7247100.73	6962941.847	6004773.037	5628269.372	5115711.55	4157093.959	4277782.634
8655695.165	8191871.92	8181479.814	7205785.905	9086474.743	6004773.037	5546479.624	5151933.037	4096946.921	4249896.144
8457061.231	7177102.43	-5822749.43	-4509290.791	-3339196.781	-2378154.925	-1708707.425	-1173085.039	-793287.8564	521006.2106
-747681.0091	328218.7021	-28600.84097	127713.1881	165225.1144	131903.6173	74409.99569	24480.6976	-4505.577517	-13566.54829
-747681.0091	328218.7021	-28600.84097	127713.1881	165225.1144	131903.6173	74409.99569	24480.6976	-4505.577517	-13566.54829
31997975.18	33076643.55	18498520.3	17446122.95	20003611.88	15899971.42	15243130.93	14259232.49	11608835.83	13299334.53
70547359.45	79266608.24	49420606.4	52599497.57	68400043.91	61713967.1	67060738.5	70909709.9	65031694.45	83611100.71
1.08549E+16	1.51606E+16	2.06348E+16	2.74718E+16	3.58811E+16	4.60867E+16	5.83278E+16	7.28587E+16	8.99484E+16	1.09881E+17
1.95737E+11	2.31258E+11	2.69739E+11	3.11181E+11	3.55582E+11	4.02944E+11	4.53266E+11	5.06547E+11	5.62789E+11	6.21991E+11
0.67711627	0.643767377	0.344037171	0.317347664	0.361095147	0.287470949	0.277669843	0.262702037	0.216833827	0.252232874

0.215	0.225	0.235	0.245	0.255	0.265	0.275	0.285	0.295
0.284560561	0.255517897	0.230300437	0.20832226	0.189092937	0.172203093	0.157311091	0.144131448	0.132425041
1.350884841	1.413716694	1.476548547	1.5393804	1.602212253	1.665044106	1.727875959	1.790707813	1.853539666

3644397.78	3460415.764	2930698.678	2903243.979	2308920.987	2527026.13	1757041.807	2133580.863	1871762.093
3644397.78	3460415.764	2930698.678	2903243.979	2308920.987	2527026.13	1757041.807	2133580.863	1871762.093
3695430.544	3161154.996	3236647.293	2286133.793	2730370.637	2444927.525	1705474.785	2142748.593	1858654.228
-336785.3498	-212247.683	-131371.8518	-79699.21155	-46752.21326	27558.58008	-15799.0342	-8766.895854	-68026.3967
-10887.6416	-4813.348384	330.6256755	-1281.294004	-1108.867125	-387.057567	68.02968669	-153.3675154	1023.586773
-10887.6416	-4813.348384	330.6256755	-1281.294004	-1108.867125	-387.057567	68.02968669	-153.3675154	1023.586773
10625665.47	9860112.145	8967334.047	8010359.952	7299242.664	7525764.25	5203895.425	6400836.688	5536199.192
74681223.75	77177467.78	77875093.78	76903543.04	77202700.02	87405680.46	66160566.1	88819432.19	83612572.61
1.32955E+17	1.59485E+17	1.898E+17	2.24243E+17	2.63173E+17	3.06964E+17	3.56005E+17	4.10699E+17	4.71464E+17
6.84153E+11	7.49276E+11	8.17358E+11	8.88401E+11	9.62403E+11	1.03937E+12	1.11929E+12	1.20217E+12	1.28801E+12
0.204813115	0.193254418	0.178751584	0.16240012	0.150491211	0.157759391	0.110884462	0.13859443	0.121771773

RAO (Heave)	K=		1.48E+11		M=		182202457.5		C=		519340252
	0.025	0.035	0.045	0.055	0.065	0.075	0.085	0.095	0.105		
H	1.11799E-84	1.31025E-21	9.96905E-08	0.001946209	0.077988626	0.358557441	0.68495789	0.88177653	0.93837707		
ω	0.157079633	0.219911486	0.282743339	0.345575192	0.408407045	0.471238898	0.53407075	0.5969026	0.65973446		

F.HULL 1	1.77762E-78	-1.9583E-15	-0.13735544	-2429.59433	85901.66154	343244.8445	-555421.98	-593788.46	-510537.74		
F.HULL 2	1.77762E-78	-1.9583E-15	-0.13735544	-2429.59433	85901.66154	343244.8445	-555421.98	-593788.46	-510537.74		
F.HULL 3	1.78187E-78	1.96196E-15	-0.13728616	-2431.49143	-86231.2119	-340555.062	557151.631	585122.82	515266.658		
PNT00N4	-1.7552E-78	3.79802E-15	0.440084457	11642.5169	-575177.739	-3072994.18	-6350975.8	-8581082.2	-9140979.6		
PNT00N5	-1.7551E-78	3.76633E-15	-0.43047845	11039.01681	-530122.52	-2630823.12	-4901171.1	-5626153	-4702239.4		
PNT00N6	-1.7551E-78	3.76633E-15	-0.43047845	11039.01681	-530122.52	-2630823.12	-4901171.1	-5626153	-4702239.4		
TOTAL	7.17549E-80	9.37605E-15	0.832869486	26429.87043	1549850.666	7988705.793	16707010.4	20435842.3	19051267.1		
F/(H/2)	128363.8785	14311796.47	16709106.95	27160361.2	39745556.62	44560256.57	48782591.7	46351522.6	40604716		
$(K-M\omega^2)^2$	2.19115E+22	2.19103E+22	2.19086E+22	2.19064E+22	2.19039E+22	2.19009E+22	2.1897E+22	2.1894E+22	2.1889E+22		
$(C\omega)^2$	6.65493E+15	1.30437E+16	2.1562E+16	3.22099E+16	4.49874E+16	5.98944E+16	7.6931E+16	9.6097E+16	1.1739E+17		
RAO	8.67174E-05	0.009668746	0.011288754	0.01835056	0.026855149	0.030110369	0.03296605	0.03132592	0.02744469		

0.115	0.125	0.135	0.145	0.155	0.165	0.175	0.185	0.195	0.205
0.907134595	0.834566895	0.748615675	0.663357019	0.584900557	0.515279512	0.454606713	0.40217997	0.357020863	0.318123656
0.72256631	0.785398163	0.848230016	0.91106187	0.973893723	1.036725576	1.099557429	1.162389282	1.225221135	1.288052988

MAXIMUM TOTAL FORCE

-393355.617	274073.6941	190556.2351	-122968.382	-78593.7434	-49123.56893	-29473.65968	17436.5868	-9851.436244	5485.751323
-393355.617	274073.6941	190556.2351	-122968.382	-78593.7434	-49123.56893	-29473.65968	17436.5868	-9851.436244	5485.751323
396201.523	271611.964	-193160.29	126811.775	-80838.0499	-50092.01628	-30793.38058	18260.62248	-10093.92264	-5965.740294
-8274968.63	7177102.43	-5846471.72	4492661.503	-3308870.73	-2396945.392	-1708707.425	-1173085.039	-792422.3965	-521954.2505
-2995542.43	1312655.617	114561.5812	509007.7633	-659143.542	-491050.6401	297587.5173	97495.0646	-18005.65257	54362.53401
-2995542.43	1312655.617	114561.5812	509007.7633	-659143.542	-491050.6401	297587.5173	97495.0646	-18005.65257	54362.53401
14656563.21	10622173.02	5429396.38	5391552.041	4865183.356	3527385.827	1203273.09	924961.1142	858230.4968	408223.4201
32313976.98	25455534.08	14505163.5	16255355.37	16635933.41	13691154.98	5293688.179	4599737.35	4807733.029	2566444.917
2.18847E+22	2.18796E+22	2.18741E+22	2.18681E+22	2.18617E+22	2.18549E+22	2.18477E+22	2.18401E+22	2.1832E+22	2.18235E+22
1.40818E+17	1.66373E+17	1.94058E+17	2.23872E+17	2.55816E+17	2.89889E+17	3.26092E+17	3.64424E+17	4.04886E+17	4.47478E+17
0.02184331	0.0172092	0.009807442	0.010992296	0.011251287	0.009261096	0.003581394	0.003112451	0.003253792	0.001737263

0.215	0.225	0.235	0.245	0.255	0.265	0.275	0.285	0.295
0.284560561	0.255517897	0.230300437	0.20832226	0.189092937	0.172203093	0.157311091	0.144131448	0.132425041
1.350884841	1.413716694	1.476548547	1.5393804	1.602212253	1.665044106	1.727875959	1.790707813	1.853539666

-3042.537676	-1605.66141	822.7995521	-406.2844338	-193.9730641	-88.70934785	-38.01367415	16.23533704	-6.458033748
-3042.537676	-1605.66141	822.7995521	-406.2844338	-193.9730641	-88.70934785	-38.01367415	16.23533704	-6.458033748
3321.068628	-1792.103372	959.5825475	-454.3138781	-246.6731266	-120.0495786	-55.84784829	25.83089725	-11.58469506
-331947.7395	-211851.6503	-129995.226	-79795.13098	-46471.61396	27660.48481	-15799.0342	-8849.532713	-68007.99682
-43504.61445	-19250.00432	-1326.065433	-5165.372195	4433.135997	1543.503278	-272.0708633	-610.7258061	4089.374154
-43504.61445	-19250.00432	-1326.065433	-5165.372195	4433.135997	1543.503278	-272.0708633	-610.7258061	4089.374154
421720.9751	255355.0851	130042.1752	91392.75812	38239.96122	30450.02309	16475.05112	10012.68275	59853.74927
2964015.627	1998725.63	1129326.345	877417.1135	404456.7896	353652.4531	209458.2269	138938.2108	903964.2151
2.18146E+22	2.18052E+22	2.17954E+22	2.17852E+22	2.17746E+22	2.17636E+22	2.17521E+22	2.17402E+22	2.17279E+22
4.92199E+17	5.3905E+17	5.8803E+17	6.3914E+17	6.92379E+17	7.47748E+17	8.05247E+17	8.64875E+17	9.26633E+17
0.002006792	0.00135353	0.000764946	0.000594454	0.000274088	0.00023972	0.000142016	9.42282E-05	0.000613243

RAO (Pitch)	K= 5.05E+13			M= 8.00E+10			C= 2.00973E+11		
	0.025	0.035	0.045	0.055	0.065	0.075	0.085	0.095	0.105
H	1.11799E-84	1.31025E-21	9.96905E-08	0.001946209	0.077988626	0.358557441	0.684957886	0.881776527	0.938377066
ω	0.157079633	0.219911486	0.282743339	0.345575192	0.408407045	0.471238898	0.534070751	0.596902604	0.659734457

F.HULL 1	7770298.416	7770298.416	7770302.352	7873890.486	12857620.34	35196985.94	64918556.05	85894406.4	91174286.28
F.HULL 2	7770298.416	7770298.416	7770302.352	7873890.486	12857620.34	35196985.94	64918556.05	85894406.4	91174286.28
F.HULL 3	7770298.416	7770298.416	7770302.331	7873511.184	12938990.78	35111460.91	65954693.96	85781629.74	91044758.51
PNT00N4	0	0	0	0	0	0	0	0	0
PNT00N5	0	0	0	0	0	0	0	0	0
PNT00N6	0	0	0	0	0	0	0	0	0
TOTAL	23310895.25	23310895.25	23310907.03	23621292.16	38654231.45	105505432.8	195791806.1	257570442.5	273393331.1
F/(H/2)	4.17014E+91	3.55822E+28	4.67666E+14	24274157098	991278694	588499473.6	571690056.2	584207981.5	582693974.4
$(K \cdot M \omega^2)^2$	2.55106E+27	2.55087E+27	2.55061E+27	2.5503E+27	2.54991E+27	2.54947E+27	2.54896E+27	2.54838E+27	2.54775E+27
$(C \omega)^2$	9.96589E+20	1.95332E+21	3.22895E+21	4.82349E+21	6.73694E+21	8.96931E+21	1.15206E+22	1.43908E+22	1.75798E+22
RAO	8.25639E+79	7.04513E+16	926.0038363	0.048067164	0.001963055	0.001165522	0.001132344	0.001157268	0.001154412
RAO (Deg)	4.73091E+81	4.03686E+18	53060.01982	2.754248477	0.112483067	0.066784438	0.06488332	0.066311454	0.066147836

0.115	0.125	0.135	0.145	0.155	0.165	0.175	0.185	0.195	0.205
0.907134595	0.834566895	0.748615675	0.663357019	0.584900557	0.515279512	0.454606713	0.40217997	0.357020863	0.318123656
0.72256631	0.785398163	0.848230016	0.91106187	0.973893723	1.036725576	1.099557429	1.162389282	1.225221135	1.288052988

MAXIMUM TOTAL FORCE

83817539.06	77916891.9	65902798.23	52488599.07	44415287.12	34181178.37	28270576.17	22897139.05	17420737.51	15529543.64
83817539.06	77916891.9	65902798.23	52488599.07	44415287.12	34181178.37	28270576.17	22897139.05	17420737.51	15529543.64
88369922.53	75031199.45	66530298.08	52218805.07	44264455.89	34181178.37	27949030.47	23013679.75	17265832.61	15473602.91
0	0	0	0	0	0	0	0	0	0
0	0	0	0	0	0	0	0	0	0
0	0	0	0	0	0	0	0	0	0
256005000.7	230864983.2	198335894.5	157196003.2	133095030.1	102543535.1	84490182.8	68807957.85	52107307.63	46532690.2
564425614.5	553256988	529873742.3	473940875.7	455103106.2	398011303.6	371706710.3	342174961.6	291900631.4	292544671.2
2.54704E+27	2.54628E+27	2.54545E+27	2.54456E+27	2.5436E+27	2.54259E+27	2.5415E+27	2.54036E+27	2.53915E+27	2.53788E+27
2.10878E+22	2.49147E+22	2.90605E+22	3.35253E+22	3.83089E+22	4.34114E+22	4.88329E+22	5.45732E+22	6.06325E+22	6.70107E+22
0.001118373	0.001096407	0.001050238	0.000939539	0.000902364	0.000789322	0.000737311	0.000678885	0.000579276	0.000580699
0.064082772	0.062824112	0.060178609	0.053835609	0.051705459	0.045228123	0.042247941	0.038900107	0.033192538	0.033274069

0.215	0.225	0.235	0.245	0.255	0.265	0.275	0.285	0.295
0.284560561	0.255517897	0.230300437	0.20832226	0.189092937	0.172203093	0.157311091	0.144131448	0.132425041
1.350884841	1.413716694	1.476548547	1.5393804	1.602212253	1.665044106	1.727875959	1.790707813	1.853539666

12623648.48	10980157.4	9420849.744	8523261.409	7793399.464	8385950.493	8698186.389	9105435.934	8837198.859
12623648.48	10980157.4	9420849.744	8523261.409	7793399.464	8385950.493	8698186.389	9105435.934	8837198.859
12700229.51	10665275.8	9621222.967	8336700.064	7797344.777	8319761.505	8679661.986	8844119.704	9343405.923
0	0	0	0	0	0	0	0	0
0	0	0	0	0	0	0	0	0
0	0	0	0	0	0	0	0	0
37947526.47	32625590.61	28462922.46	25383222.88	23384143.7	25091662.49	26076034.76	27054991.57	27017803.64
266709668.4	255368339.7	247180794.6	243691892.1	247329636	291419417.5	331521885.2	375421074.9	408046746.6
2.53654E+27	2.53514E+27	2.53368E+27	2.53215E+27	2.53057E+27	2.52891E+27	2.5272E+27	2.52542E+27	2.52358E+27
7.37078E+22	8.07237E+22	8.80586E+22	9.57125E+22	1.03685E+23	1.11977E+23	1.20587E+23	1.29517E+23	1.38765E+23
0.000529556	0.000507176	0.000491056	0.00048427	0.000491653	0.000579485	0.00065945	0.000747034	0.000812249
0.030343539	0.029061211	0.028137533	0.02774869	0.028171704	0.033204464	0.037786502	0.04280506	0.046541872

APPENDIX D
RESPONSE AMPLITUDE OPERATOR (RAO)
FOR JONSWAP SPECTRUM

RAO (surge)	K= 1.88E+05			M= 199912151.3			C= 612291.8052		
	0.025	0.035	0.045	0.055	0.065	0.075	0.085	0.095	0.105
H	1.11799E-84	1.31025E-21	9.96905E-08	0.001946209	0.07798864	0.358601485	0.693958806	1.099895596	1.703150034
ω	0.157079633	0.219911486	0.282743339	0.345575192	0.408407045	0.471238898	0.534070751	0.596902604	0.659734457

F.HULL 1	407342.4957	407342.4957	407342.7238	413655.0932	736722.3279	2313505.649	4714928.033	6860203.594	8035404.148
F.HULL 2	407342.4957	407342.4957	407342.7238	413655.0932	736722.3279	2313505.649	4714928.033	6860203.594	8035404.148
F.HULL 3	407342.4957	407342.4957	407342.7226	413631.9851	741992.1494	2307563.943	4850634.703	8444919.741	14231240.07
PNT00N4	-1.78141E-78	-3.788E-15	0.441627081	11577.69196	-577637.9184	-3073371.652	-6460895.374	-10739523.37	-16601192.53
PNT00N5	-4.45385E-79	-9.10517E-17	-0.108344185	-2788.336635	132391.3236	-657902.4874	-1236090.036	-1759308.05	2131371.135
PNT00N6	-4.45385E-79	-9.10517E-17	-0.108344185	-2788.336635	132391.3236	-657902.4874	-1236090.036	-1759308.05	2131371.135
TOTAL	1222027.487	1222027.487	1222028.395	1246943.19	1902581.534	2545398.616	5347415.323	7907187.464	17963598.1
F/(H/2)	2.18611E+90	1.86533E+27	2.45165E+13	1281407244	48791247.95	14196252.51	15411333.59	14378069.15	21094557.43
$(K-M\omega^2)^2$	2.2516E+13	8.98786E+13	2.49457E+14	5.61046E+14	1.09939E+15	1.95419E+15	3.23007E+15	5.04664E+15	7.53843E+15
$(C\omega)^2$	9250317683	18130622659	29971029294	44771537587	62532147539	83252859150	1.06934E+11	1.33575E+11	1.63176E+11
RAO	4.60615E+83	1.96736E+20	1552150.314	54.09665948	1.471476523	0.321130452	0.271160811	0.202392137	0.242954652

0.115	0.125	0.135	0.145	0.155	0.165	0.175	0.185	0.195	0.205
1.297287266	0.895637389	0.752058752	0.663422118	0.584900961	0.515279513	0.454606713	0.40217997	0.357020863	0.318123656
0.72256631	0.785398163	0.848230016	0.91106187	0.973893723	1.036725576	1.099557429	1.162389282	1.225221135	1.288052988

MAXIMUM TOTAL FORCE

8190290.4	8525615.896	8098495.8	7247100.73	6962941.847	6004773.037	5628269.372	5115711.55	4157093.959	4277782.634
8190290.4	8525615.896	8098495.8	7247100.73	6962941.847	6004773.037	5628269.372	5115711.55	4157093.959	4277782.634
12203301.73	8761564.01	8181479.814	7205785.905	6936010.143	6004773.037	5546479.624	5151933.037	4096946.921	4249896.144
-12094668.72	7702327.208	5849530.393	4250959.089	3339196.781	-2378154.925	-1708707.425	-1173085.039	-793287.8564	521006.2106
-1069264.907	352235.667	28732.38581	127725.7213	165225.1144	131903.6173	74409.99569	24480.6976	-4505.577517	-13566.54829
-1069264.907	352235.667	28732.38581	127725.7213	165225.1144	131903.6173	74409.99569	24480.6976	-4505.577517	-13566.54829
14350683.99	34219594.34	30285466.58	26206397.9	24531540.85	15899971.42	15243130.93	14259232.49	11608835.83	13299334.53
22124142.23	76413947.76	80540161.29	79003690.66	83882716.87	61713967	67060738.5	70909709.9	65031694.45	83611100.71
1.08549E+16	1.51606E+16	2.06348E+16	2.74718E+16	3.58811E+16	4.60867E+16	5.83278E+16	7.28587E+16	8.99484E+16	1.09881E+17
1.95737E+11	2.31258E+11	2.69739E+11	3.11181E+11	3.55582E+11	4.02944E+11	4.53266E+11	5.06547E+11	5.62789E+11	6.21991E+11
0.212348368	0.620599365	0.560673194	0.476651637	0.442830739	0.287470948	0.277669843	0.262702037	0.216833827	0.252232874

0.215	0.225	0.235	0.245	0.255	0.265	0.275	0.285	0.295
0.284560561	0.255517897	0.230300437	0.20832226	0.189092937	0.172203093	0.157311091	0.144131448	0.132425041
1.350884841	1.413716694	1.476548547	1.5393804	1.602212253	1.665044106	1.727875959	1.790707813	1.853539666

3644397.78	3460415.764	2930698.678	2903243.979	2308920.987	2527026.13	1757041.807	2133580.863	1871762.093
3644397.78	3460415.764	2930698.678	2903243.979	2308920.987	2527026.13	1757041.807	2133580.863	1871762.093
3695430.544	3161154.996	3236647.293	2286133.793	2730370.637	2444927.525	1705474.785	2142748.593	1858654.228
-336785.3498	-212247.683	-131371.8518	-79699.21155	-46752.21326	27558.58008	-15799.0342	-8766.895854	-68026.3967
-10887.6416	-4813.348384	330.6256755	-1281.294004	-1108.867125	-387.057567	68.02968669	-153.3675154	1023.586773
-10887.6416	-4813.348384	330.6256755	-1281.294004	-1108.867125	-387.057567	68.02968669	-153.3675154	1023.586773
10625665.47	9860112.145	8967334.047	8010359.952	7299242.664	7525764.25	5203895.425	6400836.688	5536199.192
74681223.75	77177467.78	77875093.78	76903543.04	77202700.02	87405680.46	66160566.1	88819432.19	83612572.61
1.32955E+17	1.59485E+17	1.898E+17	2.24243E+17	2.63173E+17	3.06964E+17	3.56005E+17	4.10699E+17	4.71464E+17
6.84153E+11	7.49276E+11	8.17358E+11	8.88401E+11	9.62403E+11	1.03937E+12	1.11929E+12	1.20217E+12	1.28801E+12
0.204813115	0.193254418	0.178751584	0.16240012	0.150491211	0.157759391	0.110884462	0.13859443	0.121771773

RAO (HEAVE) K= 1.48E+11 M= 182202457.5 C= 519340252

	0.025	0.035	0.045	0.055	0.065	0.075	0.085	0.095	0.105
H	1.11799E-84	1.31025E-21	9.96905E-08	0.001946209	0.07798864	0.358601485	0.69395881	1.0998956	1.70315003
ω	0.157079633	0.219911486	0.282743339	0.345575192	0.408407045	0.471238898	0.53407075	0.5969026	0.65973446
F.HULL 1	1.77762E-78	-1.9583E-15	-0.13735544	-2429.59433	85901.67736	343287.0071	-562720.69	-740669.88	-926623.64
F.HULL 2	1.77762E-78	-1.9583E-15	-0.13735544	-2429.59433	85901.67736	343287.0071	-562720.69	-740669.88	-926623.64
F.HULL 3	1.78187E-78	1.96196E-15	-0.13728616	-2431.49143	-86231.2277	-340596.895	564473.069	729860.677	-935206.6
PNT00N4	-1.7552E-78	3.79802E-15	0.440084457	11642.5169	-575177.739	-3073371.65	-6434424.5	-10703892	-16591306
PNT00N5	-1.7551E-78	3.76633E-15	-0.43047845	11039.01681	-530122.52	-2631146.28	-4965582	-7017765.2	-8534690.7
PNT00N6	-1.7551E-78	3.76633E-15	-0.43047845	11039.01681	-530122.52	-2631146.28	-4965582	-7017765.2	-8534690.7
TOTAL	7.17549E-80	9.37605E-15	0.832869486	26429.87043	1549850.651	7989687.087	16926556.8	25490900.9	36449141.4
F/(H/2)	128363.8785	14311796.47	16709106.95	27160361.19	39745548.9	44560256.55	48782598.1	46351492	42802032.3
$(K-M\omega^2)^2$	2.19115E+22	2.19103E+22	2.19086E+22	2.19064E+22	2.19039E+22	2.19009E+22	2.1897E+22	2.1894E+22	2.1889E+22
$(C\omega)^2$	6.65493E+15	1.30437E+16	2.1562E+16	3.22099E+16	4.49874E+16	5.98944E+16	7.6931E+16	9.6097E+16	1.1739E+17
RAO	8.67174E-05	0.009668746	0.011288754	0.01835056	0.026855144	0.030110369	0.03296605	0.0313259	0.02892985

0.115	0.125	0.135	0.145	0.155	0.165	0.175	0.185	0.195	0.205
1.297287266	0.895637389	0.752058752	0.663422118	0.584900961	0.515279513	0.454606713	0.40217997	0.357020863	0.318123656
0.72256631	0.785398163	0.848230016	0.91106187	0.973893723	1.036725576	1.099557429	1.162389282	1.225221135	1.288052988

MAXIMUM TOTAL FORCE

-562535.302	294129.3855	191432.6525	-122980.45	-78593.7977	-49123.56901	-29473.65968	17436.5868	-9851.436244	5485.751323
-562535.302	294129.3855	191432.6525	-122980.45	-78593.7977	-49123.56901	-29473.65968	17436.5868	-9851.436244	5485.751323
566605.2128	291487.5151	192950.8847	126824.2198	-80838.1057	-50092.01636	-30793.38058	18260.62248	-10093.92264	-5965.740294
-11834578.6	7702327.208	5873360.956	4493102.401	-3308870.73	2408521.632	-1708707.425	-1178324.894	-792422.3965	-521954.2505
-4283883.92	1408708.367	115088.4815	509057.7149	-659143.542	-491050.6401	297587.5173	97495.0646	-18005.65257	54362.53401
-4283883.92	1408708.367	115088.4815	509057.7149	-659143.542	-491050.6401	297587.5173	97495.0646	-18005.65257	54362.53401
20960811.87	11399490.23	6679354.108	5392081.151	4865183.52	1278081.198	1203273.09	930200.9691	858230.4968	408223.4201
32314834.85	25455592.55	17762851.89	16255355.39	16635922.48	4960729.725	5293688.179	4625794.614	4807733.029	2566444.917
2.18847E+22	2.18796E+22	2.18741E+22	2.18681E+22	2.18617E+22	2.18549E+22	2.18477E+22	2.18401E+22	2.1832E+22	2.18235E+22
1.40818E+17	1.66373E+17	1.94058E+17	2.23872E+17	2.55816E+17	2.89889E+17	3.26092E+17	3.64424E+17	4.04886E+17	4.47478E+17
0.02184389	0.01720924	0.012010077	0.010992296	0.011251279	0.003355582	0.003581394	0.003130083	0.003253792	0.001737263

0.215	0.225	0.235	0.245	0.255	0.265	0.275	0.285	0.295
0.284560561	0.255517897	0.230300437	0.20832226	0.189092937	0.172203093	0.157311091	0.144131448	0.132425041
1.350884841	1.413716694	1.476548547	1.5393804	1.602212253	1.665044106	1.727875959	1.790707813	1.853539666

-3042.537676	-1605.66141	822.7995521	-406.2844338	-193.9730641	-88.70934785	-38.01367415	16.23533704	-6.458033748
-3042.537676	-1605.66141	822.7995521	-406.2844338	-193.9730641	-88.70934785	-38.01367415	16.23533704	-6.458033748
3321.068628	-1792.103372	959.5825475	-454.3138781	-246.6731266	113.4223194	-55.84784829	25.83089725	-11.58469506
-331947.7395	-211851.6503	-129995.226	-79795.13098	-46471.61396	27660.48481	-15799.0342	-8849.532713	-68007.99682
-43504.61445	-19250.00432	-1326.065433	-5165.372195	4433.135997	1543.503278	-272.0708633	-610.7258061	4089.374154
-43504.61445	-19250.00432	-1326.065433	-5165.372195	4433.135997	1543.503278	-272.0708633	-610.7258061	4089.374154
421720.9751	255355.0851	130042.1752	91392.75812	38239.96122	30683.49499	16475.05112	10012.68275	59853.74927
2964015.627	1998725.63	1129326.345	877417.1135	404456.7896	356364.0408	209458.2269	138938.2108	903964.2151
2.18146E+22	2.18052E+22	2.17954E+22	2.17852E+22	2.17746E+22	2.17636E+22	2.17521E+22	2.17402E+22	2.17279E+22
4.92199E+17	5.3905E+17	5.8803E+17	6.3914E+17	6.92379E+17	7.47748E+17	8.05247E+17	8.64875E+17	9.26633E+17
0.002006792	0.00135353	0.000764946	0.000594454	0.000274088	0.000241558	0.000142016	9.42282E-05	0.000613243

RAO (PITCH)	K=			M=			C=		
	0.025	0.035	0.045	0.055	0.065	0.075	0.085	0.095	0.105
H	1.11799E-84	1.31025E-21	9.96905E-08	0.001946209	0.07798864	0.358601485	0.693958806	1.099895596	1.703150034
ω	0.157079633	0.219911486	0.282743339	0.345575192	0.408407045	0.471238898	0.534070751	0.596902604	0.659734457

F.HULL 1	7770298.416	7770298.416	7770302.352	7873890.486	12857620.34	35200354.93	65669545.79	105219718.5	159150956.5
F.HULL 2	7770298.416	7770298.416	7770302.352	7873890.486	12857620.34	35200354.93	65669545.79	105219718.5	159150956.5
F.HULL 3	7770298.416	7770298.416	7770302.331	7873511.184	12938990.78	35114819.41	66719285.88	105079236.3	158916069
PNT00N4	0	0	0	0	0	0	0	0	0
PNT00N5	0	0	0	0	0	0	0	0	0
PNT00N6	0	0	0	0	0	0	0	0	0
TOTAL	23310895.25	23310895.25	23310907.03	23621292.16	38654231.45	105515529.3	198058377.5	315518673.3	477217981.9
F/(H/2)	4.17014E+91	3.55822E+28	4.67666E+14	24274157097	991278511.6	588483504.3	570807304.1	573724769	560394530.7
$(K-M\omega^2)^2$	2.55106E+27	2.55087E+27	2.55061E+27	2.5503E+27	2.54991E+27	2.54947E+27	2.54896E+27	2.54838E+27	2.54775E+27
$(C\omega)^2$	9.96589E+20	1.95332E+21	3.22895E+21	4.82349E+21	6.73694E+21	8.96931E+21	1.15206E+22	1.43908E+22	1.75798E+22
RAO	8.25639E+79	7.04513E+16	926.0038363	0.048067164	0.001963055	0.001165491	0.001130596	0.001136502	0.001110234
RAO (Deg)	4.73091E+81	4.03686E+18	53060.01982	2.754248476	0.112483046	0.066782626	0.064783133	0.065121541	0.063616387

0.115	0.125	0.135	0.145	0.155	0.165	0.175	0.185	0.195	0.205
1.297287266	0.895637389	0.752058752	0.663422118	0.584900961	0.515279513	0.454606713	0.40217997	0.357020863	0.318123656
0.72256631	0.785398163	0.848230016	0.91106187	0.973893723	1.036725576	1.099557429	1.162389282	1.225221135	1.288052988

MAXIMUM TOTAL FORCE

116527897.1	83050005.8	66170166.37	52492987.64	44415287.12	34181178.37	28270576.17	22897139.05	17420737.51	15529543.64
116527897.1	83050005.8	66170166.37	52492987.64	44415287.12	34181178.37	28270576.17	22897139.05	17420737.51	15529543.64
123035510.8	79953288.31	66800551.1	52223167.16	44264455.89	34181178.37	27949030.47	23013679.75	17265832.61	15473602.91
0	0	0	0	0	0	0	0	0	0
0	0	0	0	0	0	0	0	0	0
0	0	0	0	0	0	0	0	0	0
356091305	246053299.9	199140883.8	157209142.4	133095030.1	102543535.1	84490182.8	68807957.85	52107307.63	46532690.2
548978340.3	549448477.3	529588635	473933980.1	455102791.9	398011302.9	371706710.3	342174961.6	291900631.4	292544671.2
2.54704E+27	2.54628E+27	2.54545E+27	2.54456E+27	2.5436E+27	2.54259E+27	2.5415E+27	2.54036E+27	2.53915E+27	2.53788E+27
2.10878E+22	2.49147E+22	2.90605E+22	3.35253E+22	3.83089E+22	4.34114E+22	4.88329E+22	5.45732E+22	6.06325E+22	6.70107E+22
0.001087765	0.001088859	0.001049672	0.000939526	0.000902363	0.000789322	0.000737311	0.000678885	0.000579276	0.000580699
0.062328947	0.062391644	0.060146229	0.053834825	0.051705423	0.045228123	0.042247941	0.038900107	0.033192538	0.033274069

0.215	0.225	0.235	0.245	0.255	0.265	0.275	0.285	0.295
0.284560561	0.255517897	0.230300437	0.20832226	0.189092937	0.172203093	0.157311091	0.144131448	0.132425041
1.350884841	1.413716694	1.476548547	1.5393804	1.602212253	1.665044106	1.727875959	1.790707813	1.853539666

12623648.48	10980157.4	9420849.744	8523261.409	7793399.464	8385950.493	8698186.389	9105435.934	8837198.859
12623648.48	10980157.4	9420849.744	8523261.409	7793399.464	8385950.493	8698186.389	9105435.934	8837198.859
12700229.51	10665275.8	9621222.967	8336700.064	7797344.777	8319761.505	8679661.986	8844119.704	9343405.923
0	0	0	0	0	0	0	0	0
0	0	0	0	0	0	0	0	0
0	0	0	0	0	0	0	0	0
37947526.47	32625590.61	28462922.46	25383222.88	23384143.7	25091662.49	26076034.76	27054991.57	27017803.64
266709668.4	255368339.7	247180794.6	243691892.1	247329636	291419417.5	331521885.2	375421074.9	408046746.6
2.53654E+27	2.53514E+27	2.53368E+27	2.53215E+27	2.53057E+27	2.52891E+27	2.5272E+27	2.52542E+27	2.52358E+27
7.37078E+22	8.07237E+22	8.80586E+22	9.57125E+22	1.03685E+23	1.11977E+23	1.20587E+23	1.29517E+23	1.38765E+23
0.000529556	0.000507176	0.000491056	0.00048427	0.000491653	0.000579485	0.00065945	0.000747034	0.000812249
0.030343539	0.029061211	0.028137533	0.02774869	0.028171704	0.033204464	0.037786502	0.04280506	0.046541872

APPENDIX E

WAVE PROFILE IN SURGE FOR

PM AND JONSWAP SPECTRUM

PM SPECT
(SURGE)

D	0.8
Hass	6.4
d	1000
Tp	12.5
Y	3.3
ω_p	0.246699
τ	0.09
g	9.80665
α	0.0081

Ts	8.6
L	115.4351
k	0.05443

RAO									0.321238	0.277716	0.291841	0.424578	0.677116	0.643767	0.344037	0.317348	0.361095	0.287471	0.27767	0.262702
ξ	5.752737	0.382838	0.970714	5.651772	3.788834	5.417551	4.131891	4.954247	5.880073	3.134893	4.4384	0.292721	3.203712	4.101431	1.832107	2.441733	1.315328	2.449192	5.804566	
f(n)	0.005	0.015	0.025	0.035	0.045	0.055	0.065	0.075	0.085	0.095	0.105	0.115	0.125	0.135	0.145	0.155	0.165	0.175	0.185	
H(f)	0	0	1.12E-84	1.31E-21	9.97E-08	0.001946	0.077989	0.358557	0.684958	0.881777	0.938377	0.907135	0.834567	0.748616	0.663357	0.584901	0.51528	0.454607	0.40218	
t	2*pi*f(n)t																			
0	0	0	-3.8E-85	-4.6E-22	4.4E-08	-0.00051	0.026195	-0.00493	-0.08062	0.126969	0.083056	-0.30426	0.267448	0.089371	0.011056	0.069223	-0.02963	0.041727	-0.04254	
1	0	0	-4.4E-85	-3.5E-22	4.8E-08	-0.0002	0.035512	-0.021654	-0.04371	0.093292	0.176604	-0.25589	0.171293	0.128648	-0.07593	-0.02705	-0.07351	-0.02325	0.011853	
2	0	0	-4.9E-85	-2.2E-22	4.97E-08	0.000138	0.038988	0.043521	0.005375	0.027352	0.196033	-0.07964	-0.0251	0.080782	-0.10414	-0.09963	-0.04521	-0.06284	0.05195	
3	0	0	-5.3E-85	-8.1E-23	4.67E-08	0.000456	0.036051	0.055901	0.052965	-0.04805	0.133189	0.136417	-0.20694	-0.0218	-0.05172	-0.08495	0.027481	-0.03381	0.02941	
4	0	0	-5.5E-85	6.3E-23	4E-08	0.00072	0.027184	0.056096	0.085803	-0.10683	0.014447	0.284293	-0.26745	-0.10962	0.040739	0.004131	0.073188	0.032142	-0.02859	
5	0	0	-5.6E-85	2.04E-22	3.01E-08	0.000899	0.013845	0.044062	0.094744	-0.12867	-0.11036	0.290086	-0.17129	-0.12318	0.101657	0.089597	0.047031	0.06299	-0.05212	
6	0	0	-5.5E-85	3.35E-22	1.78E-08	0.000972	-0.00177	0.022444	0.077297	-0.10601	-0.18885	0.1509	0.025204	-0.0533	0.088373	0.096591	-0.02531	0.025052	-0.01281	
7	0	0	-5.4E-85	4.49E-22	4.12E-09	0.00093	-0.0171	-0.0041	0.038322	-0.04668	-0.18808	-0.0637	0.206937	0.052682	0.001156	0.018998	-0.0728	-0.04024	0.014947	
8	0	0	-5.1E-85	5.43E-22	-9.9E-09	0.000778	-0.02961	-0.02974	-0.01133	0.028784	-0.10838	-0.24647	0.267448	0.122982	-0.08246	-0.07525	-0.0488	-0.06159	0.046129	
9	0	0	-4.6E-85	6.1E-22	-2.3E-08	0.000534	-0.03725	-0.04889	-0.05782	0.094297	0.016812	-0.30605	0.171293	0.109977	-0.10223	-0.10358	0.023108	-0.01568	-0.00531	
10	0	0	-4.1E-85	6.47E-22	-3.5E-08	0.000227	-0.03877	-0.05738	-0.08821	0.127198	0.134944	-0.21268	-0.022477	0.04286	-0.04119	0.072331	0.047354	-0.05034		
11	0	0	-3.4E-85	6.54E-22	-3.4E-08	-0.00011	-0.0339	-0.05337	-0.09403	0.116109	0.196441	-0.01302	-0.20694	-0.08025	0.049692	0.05727	0.05053	0.058677	-0.03468	
12	0	0	-2.7E-85	6.29E-22	-4.8E-08	-0.00043	-0.02347	-0.03772	-0.03767	0.064866	0.175494	0.193155	-0.26745	-0.12862	0.103774	0.105573	-0.02089	0.005924	0.022797	
13	0	0	-1.9E-85	5.73E-22	-5E-08	-0.0007	-0.00917	-0.01385	-0.03278	-0.06881	0.080894	0.302791	-0.17129	-0.08986	0.077516	0.061411	-0.07179	-0.0533	0.052789	
14	0	0	-1.8E-85	4.91E-22	-4.7E-08	-0.00089	0.006639	0.013039	0.017234	-0.07944	-0.04766	0.261099	0.025204	0.009763	-0.00875	-0.03654	-0.05221	-0.05432	0.019133	
15	0	0	-1.6E-86	3.84E-22	-4.1E-08	-0.00097	0.021353	0.037085	0.062448	-0.1226	-0.15621	0.088915	0.206937	0.102775	-0.08825	-0.10248	0.018644	0.003979	-0.03759	
16	0	0	7.13E-86	2.59E-22	-3.1E-08	-0.00094	0.032555	0.053046	0.09027	-0.12335	-0.1392	-0.12771	0.267448	0.126169	-0.09942	-0.07867	0.071188	0.057931	-0.04899	
17	0	0	1.57E-85	1.21E-22	-1.9E-08	-0.0008	0.038402	0.057445	0.09295	-0.08145	-0.15859	-0.2805	0.171293	0.064099	-0.03362	0.010403	0.053831	0.048621	-0.0013	
18	0	0	2.39E-85	-2.2E-23	-5.7E-09	-0.00056	0.037932	0.049321	0.069742	-0.01138	-0.05142	-0.29311	-0.0252	-0.04139	0.058204	0.094459	-0.01638	-0.01378	0.047942	
19	0	0	3.15E-85	-1.6E-22	8.36E-09	-0.00026	0.031223	0.030446	0.02711	0.062629	0.077328	-0.15923	-0.20694	-0.11884	0.104971	0.092145	-0.07051	-0.06114	0.039402	
20	0	0	3.84E-85	-3E-22	2.17E-08	7.7E-05	0.019377	0.004934	-0.02307	0.114976	0.173622	0.054233	-0.26745	-0.11579	0.070471	0.009127	-0.0554	-0.04173	0.01664	
21	0	0	4.42E-85	-4.2E-22	3.34E-08	0.000401	0.004345	-0.02165	-0.06683	0.127561	0.197049	0.24059	-0.17129	-0.03431	-0.01859	-0.08188	0.014107	0.023249	-0.05262	
22	0	0	4.9E-85	-5.2E-22	2.24E-08	0.000678	-0.0114	-0.04352	-0.09197	0.09603	0.137776	0.306705	0.025204	0.070415	-0.09325	-0.10118	0.069764	0.062837	-0.02515	
23	0	0	5.26E-85	-5.9E-22	4.8E-08	0.000874	-0.02527	-0.0559	-0.0915	0.031288	0.02068	0.219536	0.206937	0.127443	-0.09573	-0.03186	0.065919	0.033805	0.032644	
24	0	0	5.49E-85	-6.4E-22	4.98E-08	0.000967	-0.03499	-0.0561	-0.06554	-0.04427	-0.10509	0.022647	0.267448	0.098143	-0.02409	0.065366	-0.01182	-0.03214	0.051082	
25	0	0	5.59E-85	-6.6E-22	4.77E-08	0.000946	-0.03895	-0.04406	-0.02133	-0.10453	-0.18676	-0.18556	0.171293	0.002364	0.066199	0.10534	-0.06895	-0.06299	0.007931	
26	0	0	5.54E-85	-6.4E-22	4.18E-08	0.000813	-0.0365	-0.02242	0.028821	-0.12863	-0.19005	-0.30103	-0.0252	-0.09502	0.105235	0.053054	-0.05814	-0.02505	-0.04478	
27	0	0	5.36E-85	-5.9E-22	3.25E-08	0.000584	-0.02805	0.004103	0.070947	-0.10824	-0.11357	-0.26605	-0.20694	-0.12804	0.0628	-0.0457	0.009514	0.040243	-0.0435	
28	0	0	5.05E-85	-5.2E-22	2.07E-08	0.000285	-0.01498	0.029735	0.093313	-0.05043	0.010569	-0.0981	-0.26745	-0.07433	-0.02825	-0.10443	0.068065	0.061592	0.01023	
29	0	0	4.62E-85	-4.2E-22	7.23E-09	-4.7E-05	0.000546	0.048885	0.08969	0.02483	0.130274	0.11887	-0.17129	0.02973	-0.09743	-0.07169	0.059782	0.015681	0.051627	
30	0	0	4.07E-85	-3E-22	-6.8E-09	-0.00037	0.015986	0.057379	0.061087	0.0915	0.195305	0.276436	0.025204	0.113647	-0.09118	0.02383	-0.0072	-0.04735	0.030777	
31	0	0	3.42E-85	-1.6E-22	-2E-08	-0.00066	0.028797	0.053365	0.01547	0.126526	0.178368	0.295846	0.206937	0.120583	-0.01434	0.098483	-0.06711	-0.05868	-0.02718	
32	0	0	2.68E-85	-1.9E-23	-3.2E-08	-0.00086	0.03687	0.037718	-0.03446	0.117794	0.086572	0.167398	0.267448	0.045838	0.073606	0.068881	-0.06113	-0.00592	-0.05237	
33	0	0	1.88E-85	1.24E-22	-4.2E-08	-0.00096	0.038879	0.013849	-0.07478	0.068324	-0.04156	-0.04471	0.171293	-0.05996	0.104566	-0.00081	0.004883	0.053298	-0.01441	
34	0	0	1.04E-85	2.61E-22	-4.8E-08	-0.00095	0.034493	-0.01304	-0.09428	-0.00477	-0.15225	-0.23448	-0.0252	-0.12514	0.054572	-0.0878	0.066097	0.054318	0.040918	
35	0	0	1.63E-86	3.86E-22	-5E-08	-0.00083	0.024432	-0.03708	-0.08753	-0.07622	-0.19904	-0.30705	-0.20694	-0.10555	-0.03767	-0.09778	0.062409	-0.00398	0.046915	
36	0	0	-7.1E-86	4.92E-22	-4.8E-08	-0.00061	0.010353	-0.05305	-0.05744	-0.00955	-0.12444	-0.05744	-0.03226	-0.17129	0.086415	-0.08583	0.072881	-0.06501	-0.04862	
37	0	0	-1.6E-85	5.75E-22	-4.3E-08	-0.00031	-0.00543	-0.05744	-0.00955	-0.12444	-0.05744	-0.03226	-0.17129	0.086415	-0.08583	0.072881	-0.06501	-0.04862	-0.04982	
38	0	0	-2.4E-85	6.29E-22	-3.4E-08	1.6E-05	-0.02032	-0.04932	0.039954	-0.08454	0.071523	0.177781	0.025204	0.128765	-0.00446	0.104172	-0.06363	0.013784	-0.03592	
39	0	0	-3.2E-85	6.54E-22	-2.2E-08	0.000345	-0.03187	-0.03045	0.078327	-0.0154	0.170469	0.298968	0.206937	0.083893	0.080361	0.044225	0.000233	0.061136	0.021289	
40	0	0	-3.8E-85	6.47E-22	-8.8E-09	0.000632	-0.03817	-0.00493	0.094885	0.059067	0.19787	0.270737	0.267448	-0.01781	0.102968	-0.05446	0.063868	0.041727	0.052826	

[illegible]

Ts	8.6
L	115.4351
k	0.05443

[illegible]

APPENDIX F

WAVE PROFILE IN HEAVE FOR

PM AND JONSWAP SPECTRUM

at x= 54.85

PM SPECT
(HEAVE)

D	0.8
Hass	6.4
d	1000
Tp	12.5
γ	3.3
ω_0	0.246699
τ	0.09
g	9.80665
α	0.0081
Ts	8.6
L	115.4351
k	0.05443

RAO								0.03011	0.032966	0.031326	0.027445	0.021843	0.017209	0.009807	0.010992	0.011251	0.009261	0.003581	0.003112
ξ	5.752737	0.382838	0.970714	5.651772	3.788834	5.417551	4.131891	4.954247	5.880073	3.134893	4.4384	0.292721	3.203712	4.101431	1.832107	2.441733	1.315328	2.449192	5.804566
f(n)	0.005	0.015	0.025	0.035	0.045	0.055	0.065	0.075	0.085	0.095	0.105	0.115	0.125	0.135	0.145	0.155	0.165	0.175	0.185
H(f)	0	0	1.12E-84	1.31E-21	9.97E-08	0.001946	0.077989	0.358557	0.684958	0.881777	0.938377	0.907135	0.834567	0.748616	0.663357	0.584901	0.51528	0.454607	0.40218
t	2*π*f(n)t																		
0	0	0	-3.8E-85	-4.6E-22	4.4E-08	-0.00051	0.026195	-0.00046	-0.00957	0.013629	0.005369	-0.00982	0.007149	0.002548	0.000383	0.002157	-0.00095	0.000538	-0.0005
1	0	0	-4.4E-85	-3.5E-22	4.88E-08	-0.0002	0.035512	0.00203	-0.00519	0.010014	0.011416	-0.00825	0.004579	0.003667	-0.00263	-0.00084	-0.00237	-0.0003	0.00014
2	0	0	-4.9E-85	-2.2E-22	4.97E-08	0.000138	0.038988	0.004079	0.000638	0.002936	0.012672	-0.00257	-0.00067	0.002303	-0.00361	-0.0031	-0.00146	-0.00081	0.00061
3	0	0	-5.3E-85	-8.1E-23	4.67E-08	0.000456	0.036051	0.00524	0.006287	-0.00516	0.008609	0.004401	-0.00553	-0.00062	-0.00179	-0.00265	0.000885	-0.00044	0.000348
4	0	0	-5.5E-85	6.3E-23	4E-08	0.00072	0.027184	0.005258	0.010185	-0.01147	0.000934	0.009171	-0.00715	-0.00312	0.001411	0.000129	0.002358	0.000415	-0.00034
5	0	0	-5.6E-85	2.04E-22	3.01E-08	0.000899	0.013845	0.00413	0.011247	-0.01381	-0.00713	0.009358	-0.00458	-0.00351	0.003521	0.002792	0.001515	0.000812	-0.00062
6	0	0	-5.5E-85	3.35E-22	1.78E-08	0.000972	-0.00177	0.002102	0.009176	-0.01138	-0.01221	0.004868	0.006674	-0.00152	0.002905	0.00301	-0.00082	0.000323	-0.00015
7	0	0	-5.4E-85	4.49E-22	4.12E-09	0.00093	-0.0171	-0.00038	0.005449	-0.00501	-0.01216	-0.00205	0.005532	0.001502	4E-05	0.000592	-0.00235	-0.00052	0.000497
8	0	0	-5.1E-85	5.43E-22	-9.9E-09	0.000778	-0.02961	-0.00279	-0.00134	0.00309	-0.00701	-0.00795	0.007149	0.003506	-0.00286	-0.00234	-0.00157	-0.00079	0.000547
9	0	0	-4.6E-85	6.1E-22	-2.3E-08	0.000534	-0.03725	-0.00458	-0.00686	0.010122	0.001087	-0.00987	0.004579	0.003135	-0.00354	-0.00323	0.000744	-0.0002	-6.3E-05
10	0	0	-4.1E-85	6.47E-22	-3.5E-08	0.000227	-0.03877	-0.00538	-0.01047	0.013653	0.008723	-0.00686	-0.00067	0.000641	-0.00148	-0.00128	0.00223	0.000611	-0.0006
11	0	0	-3.4E-85	6.54E-22	-4.3E-08	-0.00011	-0.0339	-0.005	-0.01116	0.012463	0.012698	-0.00042	-0.00553	-0.00229	0.001721	0.001784	0.001628	0.000757	-0.00041
12	0	0	-2.7E-85	6.29E-22	-4.8E-08	-0.00043	-0.02347	-0.00354	-0.00874	0.006963	0.011344	0.006331	-0.00715	-0.00367	0.003595	0.00329	-0.00067	7.64E-05	0.00027
13	0	0	-1.9E-85	7.33E-22	-5E-08	-0.0007	-0.00917	-0.0013	-0.00389	-0.00095	0.005229	0.009768	0.00458	0.00256	0.002685	0.001913	-0.00231	-0.00069	0.000625
14	0	0	-1E-85	4.91E-22	-4.7E-08	-0.00089	0.006639	0.001222	0.002046	-0.00853	-0.00308	0.008423	0.000674	0.000278	-0.0003	-0.00114	-0.00168	-0.0007	0.000227
15	0	0	-1.6E-86	3.84E-22	-4.1E-08	-0.00097	0.012153	0.003476	0.007413	-0.01316	-0.0101	0.002868	0.005532	0.00293	-0.00306	-0.00319	0.000601	5.13E-05	-0.00045
16	0	0	7.13E-86	2.59E-22	-3.1E-08	-0.00094	0.032555	0.004972	0.010715	-0.01324	-0.01288	-0.00412	0.007149	0.003597	-0.00344	-0.00245	0.002293	0.000747	-0.00058
17	0	0	1.57E-85	1.21E-22	-1.9E-08	-0.0008	0.038402	0.005384	0.011034	-0.00874	-0.01025	-0.00905	0.004579	0.001827	-0.00116	0.000438	0.001734	0.000627	-1.6E-05
18	0	0	2.39E-85	-2.2E-23	-5.7E-09	-0.00056	0.037932	0.004623	0.008279	-0.01122	-0.00332	-0.00946	-0.00067	-0.00118	0.002016	0.002943	-0.00053	-0.00018	0.000568
19	0	0	3.15E-85	-1.6E-22	8.36E-09	-0.00026	0.013223	0.002854	0.003218	0.006722	0.004998	-0.00514	-0.00553	-0.00339	0.003636	0.002841	-0.00227	-0.00079	0.000467
20	0	0	3.84E-85	-3E-22	2.17E-08	7.7E-05	0.019377	0.000462	-0.00274	0.012341	0.011223	0.00175	-0.00715	-0.0033	0.002441	0.000284	-0.00178	-0.00054	-0.0002
21	0	0	4.42E-85	-4.2E-22	3.34E-08	0.000401	0.004345	-0.00203	-0.00793	0.013692	0.012737	0.007761	-0.00458	-0.00098	-0.00064	-0.00255	0.000454	0.0003	-0.00062
22	0	0	4.9E-85	-5.2E-22	4.24E-08	0.000678	-0.0114	-0.00408	-0.01092	0.010308	0.008906	0.009894	0.000674	0.002007	-0.00323	-0.00315	0.002247	0.00081	-0.0003
23	0	0	5.26E-85	-5.9E-22	4.8E-08	0.000874	-0.02527	-0.00524	-0.01086	0.003358	0.001337	0.007082	0.005532	0.003633	-0.00332	-0.00099	0.001834	0.000436	0.000387
24	0	0	5.49E-85	-6.4E-22	4.98E-08	0.000967	-0.03499	-0.00526	-0.00778	-0.00475	-0.00679	0.000731	0.007149	0.002798	-0.00293	0.002037	-0.00308	-0.00041	0.000605
25	0	0	5.59E-85	-6.6E-22	4.77E-08	0.000946	-0.03895	-0.00413	-0.00253	-0.01122	-0.01207	-0.00599	0.004579	6.74E-05	0.000283	0.003282	-0.00222	-0.00081	9.4E-05
26	0	0	5.54E-85	-6.4E-22	4.18E-08	0.000813	-0.0365	-0.0021	0.003421	-0.01381	-0.01228	-0.00971	-0.00067	-0.00271	0.003645	0.001653	-0.00188	-0.00032	-0.00053
27	0	0	5.36E-85	-5.9E-22	3.25E-08	0.000584	-0.02805	0.000385	0.008422	-0.01162	-0.00734	-0.00858	-0.00553	-0.00365	0.002175	-0.00142	0.000306	0.000519	-0.00052
28	0	0	5.05E-85	-5.2E-22	2.07E-08	0.000285	-0.01498	0.002787	0.011077	-0.00541	0.000683	-0.00316	-0.00715	-0.00212	-0.00098	-0.00325	0.002193	0.000794	0.000121
29	0	0	4.62E-85	-4.2E-22	7.23E-09	-4.7E-05	0.000546	0.004582	0.010647	0.002665	0.008421	0.003835	-0.00458	0.000848	-0.00337	-0.00223	0.001926	0.000202	0.000612
30	0	0	4.07E-85	-3E-22	-6.8E-09	-0.00037	0.015986	0.005378	0.007251	0.008822	0.012625	0.008918	0.000674	0.00324	-0.00316	0.000743	-0.00023	-0.00061	0.000365
31	0	0	3.42E-85	-1.6E-22	-2E-08	-0.00066	0.028797	0.005002	0.001836	0.013581	0.01153	0.009544	0.005532	0.003437	-0.0005	0.003069	-0.00216	-0.00076	-0.00032
32	0	0	2.68E-85	-1.9E-23	-3.2E-08	-0.00086	0.03687	0.003535	-0.00409	0.012644	0.005596	0.0054	0.007149	0.001307	0.00255	0.002707	-0.00197	-7.6E-05	-0.00062
33	0	0	1.88E-85	1.24E-22	-4.2E-08	-0.00096	0.038879	0.001298	-0.00888	0.007334	-0.00269	-0.00144	0.004579	-0.00171	0.003622	-2.5E-05	0.000157	0.000587	-0.00017
34	0	0	1.04E-85	2.61E-22	-4.8E-08	-0.00095	0.034493	-0.00122	-0.01119	-0.00051	-0.00984	-0.00756	-0.00067	-0.00357	0.00189	-0.00274	0.002129	0.000701	0.000485
35	0	0	1.63E-86	3.86E-22	-5E-08	-0.00083	0.024432	-0.00348	-0.01039	-0.00818	-0.01287	-0.00991	-0.00553	-0.00301	-0.0013	-0.00305	0.002011	-5.1E-05	0.000556
36	0	0	-7.1E-86	4.92E-22	-4.8E-08	-0.00061	0.010353	-0.00497	-0.00669	-0.01302	-0.01049	-0.0073	-0.00715	-0.00041	-0.00349	-0.00069	-8.2E-05	-0.00075	-4.3E-05
37	0	0	-1.6E-85	5.75E-22	-4.3E-08	-0.00031	-0.00543	-0.00538	-0.01013	-0.01336	-0.00371	-0.01004	-0.00458	0.002463	-0.00297	0.002271	-0.00209	-0.00063	-0.00059
38	0	0	-2.4E-85	6.29E-22	-3.4E-08	1.6E-05	-0.02032	-0.00462	0.004743	-0.00907	0.004623	0.005735	0.000674	0.003671	-0.00015	0.003246	-0.00205	0.000178	-0.00043
39	0	0	-3.2E-85	6.54E-22	-2.2E-08	0.000345	-0.03187	-0.00285	0.009298	-0.00165	0.011019	0.009645	0.005532	0.002392	0.002784	0.001378	7.5E-06	0.000789	0.000252
40	0	0	-3.8E-85	6.47E-22	-8.8E-09	0.000632	-0.03817	-0.00046	0.011263	0.00634	0.010179	0.008734	0.007149	-0.00051	0.003567	-0.0017	0.002058	0.000538	0.000626

[illegible]

[illegible]

APPENDIX G

WAVE PROFILE IN PITCH FOR

PM AND JONSWAP SPECTRUM

D	0.8
Hass	6.4
d	1000
TP	12.5
γ	3.3
ω_0	0.246699
τ	0.09
β	9.80665
α	0.0081
Ts	8.6
L	115.4351
k	0.05443

RAO									0.066784	0.064883	0.066311	0.066148	0.064083	0.062824	0.060179	0.053836	0.051705	0.045228	0.042248	0.0389
f	5.752737	0.382838	0.970714	5.651772	3.788834	5.417551	4.131891	4.954247	5.880073	3.134893	4.4384	0.292721	3.203712	4.101431	1.832107	2.441733	1.315328	2.449192	5.804566	
f(n)	0.005	0.015	0.025	0.035	0.045	0.053	0.065	0.075	0.085	0.095	0.105	0.115	0.125	0.135	0.143	0.155	0.165	0.175	0.185	
H(f)	0	0	1.12E-84	1.31E-21	9.97E-08	0.001946	0.077989	0.358557	0.684958	0.881777	0.938377	0.907135	0.834567	0.748616	0.663357	0.584901	0.51528	0.454607	0.40218	
t	2*pi*f(n)t																			
0	0	0	-3.8E-85	-4.6E-22	4.4E-08	-0.00051	0.026195	-0.00103	-0.01884	0.028849	0.01294	-0.02879	0.0261	0.015633	0.001876	0.009912	-0.00466	0.006349	-0.0063	
1	0	0	-4.4E-85	-3.5E-22	4.88E-08	-0.0002	0.035512	0.004502	-0.01021	0.021198	0.027514	-0.02422	0.016716	0.022503	-0.01288	-0.00387	-0.01157	-0.00354	0.001755	
2	0	0	-4.9E-85	-2.2E-22	4.97E-08	0.000138	0.038988	0.009048	0.001256	0.006215	0.030541	-0.00754	-0.00246	0.01413	-0.01787	-0.01427	-0.00711	-0.00956	0.007695	
3	0	0	-5.3E-85	-8.1E-23	4.67E-08	0.000456	0.036051	0.011622	0.012374	-0.01092	0.02075	0.012911	-0.02019	-0.00381	-0.00877	-0.01216	0.004324	-0.00514	0.004355	
4	0	0	-5.5E-85	6.3E-23	4E-08	0.00072	0.027184	0.011662	0.020046	-0.02427	0.002251	0.026906	-0.0261	-0.01917	0.006911	0.000591	0.011515	0.00489	-0.00423	
5	0	0	-5.6E-85	2.04E-22	3.01E-08	0.000899	0.013845	0.00916	0.022135	-0.02924	-0.01719	0.027454	-0.01672	-0.02155	0.017245	0.012829	0.007399	0.009584	-0.00772	
6	0	0	-5.5E-85	3.35E-22	1.78E-08	0.000972	-0.00177	0.004662	0.018059	-0.02409	0.014281	0.00647	-0.00932	0.014228	0.013831	-0.00398	0.003812	-0.00719		
7	0	0	-5.4E-85	4.49E-22	4.12E-09	0.00093	-0.0171	-0.00085	0.008953	-0.01061	-0.0293	-0.00603	0.020195	0.009215	0.000196	0.002719	-0.01145	-0.00612	0.006211	
8	0	0	-5.1E-85	5.43E-22	-9.9E-09	0.000778	-0.02961	-0.00618	-0.00265	0.00654	-0.01688	-0.02333	0.0261	0.021512	-0.01399	-0.01077	-0.00788	-0.00937	0.006831	
9	0	0	-4.6E-85	6.1E-22	-2.3E-08	0.000534	-0.03725	-0.01016	-0.01351	0.021426	0.002619	-0.02897	0.016716	0.019237	-0.01734	-0.01483	0.003636	-0.00239	-0.00079	
10	0	0	-4.1E-85	6.47E-22	-3.5E-08	0.000227	-0.03877	-0.01193	-0.02061	0.028902	0.021024	-0.02013	-0.00246	0.003932	-0.00727	-0.0059	0.01138	0.007205	-0.00745	
11	0	0	-3.4E-85	6.54E-22	-4.3E-08	-0.00011	-0.0339	-0.01109	-0.02197	0.026382	0.030605	-0.00123	-0.02019	-0.01404	0.00843	0.008201	0.00795	0.008928	-0.00514	
12	0	0	-2.7E-85	6.29E-22	-4.8E-08	-0.00043	-0.02347	-0.00784	-0.01721	0.014739	0.027341	0.01828	-0.0261	-0.0225	0.017605	0.015117	-0.00329	0.000901	0.003376	
13	0	0	-1.9E-85	5.73E-22	-5E-08	-0.0007	-0.00917	-0.00288	-0.00766	-0.002	0.012603	0.028656	-0.01672	-0.01572	0.01315	0.008793	-0.0113	-0.00811	0.007817	
14	0	0	-1E-85	4.91E-22	-4.7E-08	-0.00089	0.006639	0.002711	0.004026	-0.01805	-0.00742	0.024711	0.00246	0.001708	-0.00149	-0.00523	-0.00821	-0.00826	0.002833	
15	0	0	-1.6E-86	3.84E-22	-4.1E-08	-0.00097	0.021353	0.00771	0.01459	-0.02786	-0.02434	0.008415	0.020195	0.017977	-0.01497	-0.01467	0.002933	0.000605	-0.00557	
16	0	0	7.13E-86	2.59E-22	-3.1E-08	-0.00094	0.032555	0.011028	0.02109	-0.02803	-0.03103	-0.01209	0.0261	0.022069	-0.01687	-0.01127	0.0112	0.008814	-0.00725	
17	0	0	1.57E-85	1.21E-22	-1.9E-08	-0.0008	0.038402	0.011943	0.021716	-0.01851	-0.02471	-0.02655	0.016716	0.011212	-0.0057	0.002011	0.008469	0.007398	-0.0002	
18	0	0	2.39E-85	-2.2E-23	-5.7E-09	-0.00056	0.037932	0.010254	0.016294	-0.00259	-0.00801	-0.02774	-0.00246	-0.00724	0.009874	0.013526	-0.00258	-0.0021	0.007099	
19	0	0	3.15E-85	-1.6E-22	8.36E-09	-0.00026	0.031223	0.00633	0.006334	0.01423	0.012047	-0.01507	-0.02019	-0.02079	0.017807	0.013194	-0.01109	-0.0093	0.005385	
20	0	0	3.84E-85	-3E-22	2.17E-08	7.7E-05	0.019377	0.001026	-0.00539	0.026125	0.02705	0.005133	-0.0261	-0.02025	0.011955	0.001307	-0.00872	-0.00635	-0.00246	
21	0	0	4.42E-85	-4.2E-22	3.34E-08	0.000401	0.004345	-0.0045	-0.01561	0.028984	0.0307	0.02277	-0.01672	-0.006	-0.00315	-0.01173	0.002219	0.003537	-0.00779	
22	0	0	4.9E-85	-5.2E-22	4.24E-08	0.000678	-0.0114	-0.00905	-0.02149	0.02182	0.021465	0.029027	0.00246	0.012317	-0.01582	-0.01449	0.010976	0.009561	-0.00372	
23	0	0	5.26E-85	-5.9E-22	4.8E-08	0.000874	-0.02527	-0.01162	-0.02138	0.007109	0.003222	0.020777	0.020195	0.022292	-0.01624	-0.00456	0.008955	0.005144	0.004834	
24	0	0	5.49E-85	-6.4E-22	4.98E-08	0.000967	-0.03499	-0.01166	-0.01531	-0.01006	-0.01637	0.002143	0.0261	0.017167	-0.00409	0.00936	-0.00186	-0.00489	0.007564	
25	0	0	5.59E-85	-6.6E-22	4.77E-08	0.000946	-0.03895	-0.00916	-0.00498	-0.02375	-0.0291	-0.01756	0.016716	0.000414	0.01123	0.015084	-0.01085	-0.00958	0.001174	
26	0	0	5.54E-85	-6.4E-22	4.18E-08	0.000813	-0.0365	-0.00466	0.006734	-0.02923	-0.02961	-0.02849	-0.00246	-0.01662	0.017852	0.007597	-0.00918	-0.00381	-0.00663	
27	0	0	5.36E-85	-5.9E-22	3.25E-08	0.000584	-0.02805	0.000853	0.016576	-0.0246	-0.01769	-0.02518	-0.02019	-0.0224	0.010654	-0.00654	0.001497	0.006123	-0.00644	
28	0	0	5.05E-85	-5.2E-22	2.07E-08	0.000285	-0.01498	0.006182	0.021801	-0.01146	0.001647	-0.00928	-0.0261	-0.013	-0.00479	-0.01495	0.010709	0.009371	0.001515	
29	0	0	4.62E-85	-4.2E-22	7.23E-09	-4.7E-05	0.000546	0.010163	0.020954	0.005642	0.020296	0.01125	-0.01672	0.0052	-0.01653	-0.01027	0.009406	0.002386	0.007645	
30	0	0	4.07E-85	-3E-22	-6.8E-09	-0.00037	0.015986	0.011929	0.014272	0.02079	0.030428	0.026162	0.00246	0.019879	-0.01547	0.030412	-0.00113	-0.0072	0.004557	
31	0	0	3.42E-85	-1.6E-22	-2E-08	-0.00066	0.028797	0.011095	0.003614	0.028749	0.027789	0.027999	0.020195	0.021092	-0.00243	0.014102	-0.01056	-0.00893	-0.00402	
32	0	0	2.68E-85	-1.9E-23	-3.2E-08	-0.00086	0.03687	0.007842	-0.00805	0.026765	0.013488	0.015843	0.0261	0.008018	0.012487	0.012441	-0.00962	-0.0009	-0.00775	
33	0	0	1.88E-85	1.24E-22	-4.2E-08	-0.00096	0.038879	0.002879	-0.01747	0.015524	-0.00647	-0.00423	0.016716	-0.01049	0.017739	-0.00012	0.000768	0.008109	-0.00213	
34	0	0	1.04E-85	2.61E-22	-4.8E-08	-0.00095	0.034493	-0.00271	-0.02203	-0.00108	-0.02372	-0.02219	-0.00246	-0.02189	0.009258	-0.01257	0.010399	0.008265	0.006059	
35	0	0	1.63E-86	3.86E-22	-5E-08	-0.00083	0.024432	-0.00771	-0.02045	-0.01732	-0.03101	-0.02906	-0.02019	-0.01846	-0.00639	-0.01402	0.009819	-0.00061	0.006947	
36	0	0	-7.1E-86	4.92E-22	-4.8E-08	-0.00061	0.010353	-0.01103	-0.01317	-0.02756	-0.02529	-0.02141	-0.0261	-0.00253	-0.01709	-0.00318	-0.0004	-0.00881	-0.00054	
37	0	0	-1.6E-85	5.75E-22	-4.3E-08	-0.00031	-0.00543	-0.01194	-0.00223	-0.02828	-0.00895	-0.00305	-0.01672	0.015116	-0.01456	0.010436	-0.01023	-0.0074	-0.00738	
38	0	0	-2.4E-85	6.29E-22	-3.4E-08	1.6E-05	-0.02032	-0.01025	0.009335	-0.01921	0.011143	0.016825	0.00246	0.022523	-0.00076	0.014916	-0.01001	0.002097	-0.00532	
39	0	0	-3.2E-85	6.54E-22	-2.2E-08	0.000345	-0.03187	-0.00633	0.0181	-0.0035	0.026558	0.028295	0.020195	0.014674	0.013633	0.006333	3.6E-05	0.009302	0.003152	
40	0	0	-3.8E-85	6.47E-22	-8.8E-09	0.000632	-0.03817	-0.00103	0.022168	0.013421	0.030828	0.025623	0.0261	-0.00311	0.017468	-0.0078	0.010048	0.006349	0.00782	

[illegible]

[illegible]